Target Guarding Problem in probabilistic setting

A Project Report

submitted by

NAVEEN KOTHURI

in partial fulfilment of the requirements
for the award of the degree of

MASTER OF TECHNOLOGY

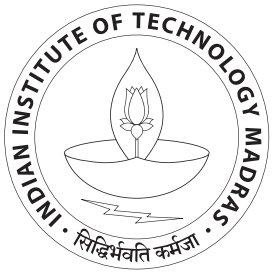

DEPARTMENT OF ELECTRICAL ENGINEERING

INDIAN INSTITUTE OF TECHNOLOGY MADRAS.

May 2018

THESIS CERTIFICATE

This is to certify that the thesis entitled **Target Guarding Problem in probabilistic setting**, submitted by **Naveen Kothuri**, to the Indian Institute of Technology, Madras, for the award of the degree of **Master of Technology**, is a bonafide record of the research work carried out by her under my supervision. The contents of this thesis, in full or in parts, have not been submitted to any other Institute or University for the award of any degree or diploma.

Prof. Bharath Bhikkaji
Research Guide
Assistant Professor
Dept. of Electrical Engineering
IIT-Madras, 600 036

Place: Chennai

Date:

ACKNOWLEDGEMENTS

My profoundest gratitude to my advisor Dr. Bharath Bhikkaji for his guidance, unparalleled support and for the freedom he granted me to explore different ways to formulate and solve the problem. His unwavering positive outlook towards research and the many hour-long discussions with him, rejuvenated my curiosity despite disappointing results.

I would like to thank Prof. P. Viswanadha Reddy for his insightful suggestions and constructive feedback which helped me deftly arrive at appropriate results.

My special thanks to Jitesh Mohanan for patiently listening to my unrefined ideas and correcting me at various stages of my project. I thank Akshit Sardagi, for lending his immense help in my work.

I thank Hari Kumar Ganesan, Sunil Kumar, Partha Paul who have been my inspiration since the day I met them, for always raising the standards.

I thank my parents and sister for holding onto me in times of despair and for many more such times to come. Finally, I would like to thank Rudolf E. Kalman for the amazing filter which made the pursuit of solution to state estimation problem easier.

ABSTRACT

KEYWORDS: Target protection games, Dominance regions, Apollonius circle, Kalman filter, zero-sum differential games, Bayesian Nash equilibrium

The target guarding problem consists of two players, evader and pursuer. Evader tries to reach a stationary target while avoiding pursuer and pursuer tries to obstruct evader from reaching the target. Optimal strategies for the players have been studied extensively in the literature. Pursuer may lose an otherwise winning game due to lack of perfect data. In this work, we try to show how these strategies translate when evader's position and velocity are not precisely known to the pursuer. The problem is formulated in game-theoretic framework and Bayesian Nash equilibrium strategies of players are determined. After studying the game geometry, two Kalman observers are designed to filter out the noise and their performances are analyzed. Also satisfactory performance of these filters are validated through experiments conducted on a developed in-house testbed. As the target guarding problem arises usually in building autonomous systems used in remote terrains, the measurement data is not always reliable. This study is important to do post-processing of the obtained measurement data before using it to make optimal decisions.

TABLE OF CONTENTS

LIST OF FIGURES

ABBREVIATIONS

TGP	Target Guarding Problem
i.i.d	identical and independent distribution (of noise)
EKF	Extended Kalman Filter
KF1	Kalman Filter with evader's position and speed as states
KF2	Kalman Filter with interception point and speed of evader as states
PID	Proportional, Integral and Differential controller
SDK	Software Development Kit
IITM	Indian Institute of Technology, Madras
PSNE	Pure Strategy Nash Equilibrium
PSBNE	Pure Strategy Bayesian Nash Equilibrium

CHAPTER 1

Introduction

Target guarding problem or asset defending problem often finds applications in border security systems where autonomous robots are employed to guard a secluded territory of interest from invaders. In its basic form, first considered by Rufus Issacs, the target guarding problem consists of two players, evader E (invader robot) and pursuer P (guard robot). Evader tries to reach the target zone C while evading the pursuer who tries to protect C by intercepting any intruder before reaching C. As the objectives of both the players are opposite, the target guarding problem is a zero-sum differential game. Pursuer wins the game if he successfully intercepts the evader before evader reaches C. Evader wins the game if he successfully evades pursuer and reaches C.

Rufus Isaacs in his pioneering work on differential games [1], solved elementary version of target guarding problem where both the players are assumed to have equal speeds. If the target zone is closer to the evader, the optimal strategy of evader is to employ pure-pursuit i.e., head towards target zone. Pursuer loses in such a game. But pursuer is usually closer to the target zone he is protecting. The optimal strategy of each of players when target zone is closer to pursuer is to head towards D, the closest point to C on the perpendicular bisector of their positions (refer Figure 1.1). Deviation from the optimal strategy causes the evader to be intercepted at farther distance from C. Evader reaches a much closer region to C if pursuer chooses to head towards any point other than D. Both players find the closest point to C on the perpendicular bisector of their instantaneous positions and head towards it.

Optimal strategies of the evader and pursuer when their speeds are not equal are presented in [2], [8]. Pontryagin's maximum principle is used in [8] to obtain the

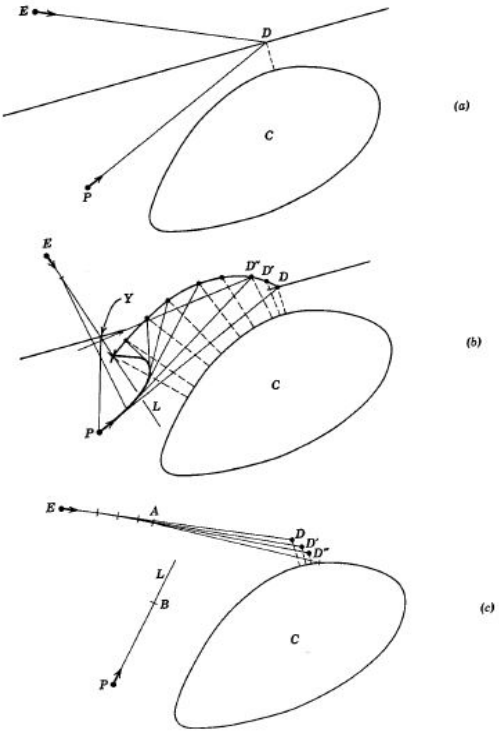

Figure 1.1: Target guarding problem. (a). Both players play optimally. (b) Only P plays optimally. (c) Only E plays optimally

optimal strategies of the players. In [2] as well, both players find the instantaneous closest point to target on the capture locus and head towards it.

Optimal strategy of each player depends on the instantaneous position and speed of other player. Decisions based on monitored actions of other player play a crucial role in determining the strategies of the player especially when the criterion for the capture is coincidence of both players. But sensor data is rarely associated with negligible noise and so it cannot be relied upon to make decisions without post-processing.

Various solutions to stochastic pursuit-evasion games have been proposed in literature but attempts to find strategies of players in stochastic version of TGP are not known. As the two problems fundamentally differ in the roles of each of players, solutions derived for stochastic pursuit-evasion games cannot be directly applied without studying game geometry. We attempt to provide a reliable strategy for the pursuer to win the game when he receives noise-corrupted data of evader's position and speed.

In this work, we assume evader always gets perfect data of the position of pursuer and plays optimally at every instant whereas pursuer gets noise corrupted data of evader's position and speed. An Extended Kalman Filter (EKF) is designed for the dynamical model describing evader's maneuver. EKF for the dynamical model of interception point/capture point is also designed after studying the game geometry. The performances of the two filters are juxtaposed and studied. The Kalman filters are implemented on the generic in-house testbed developed and respective performances are experimentally validated.

Probability density map of the interception point can be found if statistics of sensor noise at every instant are known. Strategies that can be employed by pursuer based on the knowledge of this probability density map are investigated and relevant conclusions are drawn.

1.1 Contributions of the thesis

The key contributions of this thesis are:

- TGP is formulated in game-theoretic framework and pure strategy Bayesian Nash equilbrium of the game is found.
- Two Kalman observers in an attempt to filter out the noise associated with the sensor data of evader's position, are designed.
- Probability density map of the interception point is found. Some strategies pursuer can employ based on the knowledge of probability density map of interception point are studied.
- The performance of the designed Kalman filters are validated experimentally on the developed generic testbed.

1.2 Chapter wise Descriptions

The rest of the thesis is organized as follows: Chapter 2 is dedicated to study the geometry of game under consideration. In section 2.1, target guarding problem in deterministic setting is explained. Sections 2.2 to 2.5 develop the prerequisites necessary

to model the dynamics of evader's maneuver and interception point. Game-theoretic analysis of target guarding problem is presented in chapter 3. Kalman filter design for the established models of evader's maneuver and interception point is presented in chapter 4. In section 4.1, a brief overview of EKF is given. Section 4.2 and 4.4 present two EKFs and corresponding simulation results. In chapter 5, some miscellaneous strategies are studied to check if pursuer can win the game without needing to estimate evader's position and speed. In chapter 6, experimental validation of the one of the Kalman filters is presented. Testbed setup for conducting experiments is briefly demonstrated in section 6.1. Section 6.2 presents the practical considerations which are not considered in modelling the dynamics of players. We conclude in section 6.4 with a brief on scope of future work.

CHAPTER 2

Game geometry

2.1 TGP in deterministic setting

The target guarding problem studied in [2] is explained and results are briefly reproduced in this section. We assume both the players are zero-dimensional robots. Target zone is also assumed to be a point. Constraints on turn angle rates of these robots are not considered in evaluating the optimal strategies of the players. Both players are constrained to move in a straight line.

Let evader E be at (x_e, y_e), pursuer P be at (x_p, y_p) and target T be at (x_t, y_t). Let 'k' denotes speed of E to speed of P ratio $(\frac{v_e}{v_p})$. Assume $k < 1$ for the rest of the analysis presented. The objective of E is to minimize his distance from the target at the end of the game and that of P is to maximize the same. Dominance region, R_E (R_P) of E (P) is defined as the set of all points in $\mathbb{R}^2$ which are reachable by E (P) faster than P (E). E wins the game by employing pure-pursuit strategy if $T \in R_E$. The criteria for the interception of E by P to happen are:

- $T \in R_P$
- $$\frac{\sqrt{(x-x_p)^2+(y-y_p)^2}}{v_p} = \frac{\sqrt{(x-x_e)^2+(y-y_e)^2}}{v_e} \tag{2.1}$$
  where (x, y) is the capture point I_c.

In other words, P intercepts E if P and E arrive at I_c simultaneously. Simplifying (2.1), we get the equation (2.2) for capture locus.

$$C : (x-x_c)^2 + (y-y_c)^2 = R^2 \tag{2.2}$$

where

$$x_c = \frac{x_e - x_p k^2}{1 - k^2}, y_c = \frac{y_e - y_p k^2}{1 - k^2} \tag{2.3}$$

$$R = \sqrt{x_c^2 + y_c^2 - \frac{x_e^2 + y_e^2}{1 - k^2} + k^2 \frac{x_p^2 + y_p^2}{1 - k^2}} \tag{2.4}$$

$$= \sqrt{\left(\frac{k}{1 - k^2}\right)^2 ((x_e - x_p)^2 + (y_e - y_p)^2)}$$

The capture locus is an Apollonius circle C with center (x_c, y_c) and radius R (refer Fig .2.1). C is the set of all points in $\mathbb{R}^2$ where interception of E by P can happen depending on the direction in which E moves.

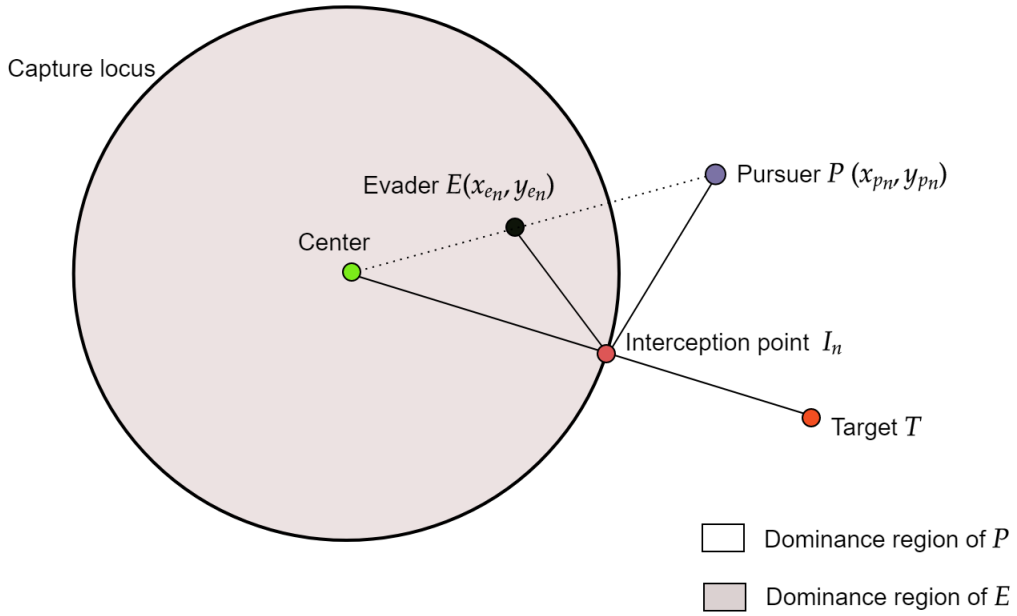

Figure 2.1: Capture locus when both E and P are moving with different speeds

If T is in P's dominance region, no matter in which direction E chooses to move, he will be intercepted by P. So the best thing for E to do is to get himself intercepted at the closest point I to T on C. Hence this is considered as optimal play for E. Assuming E plays optimally, P not pursuing I implies that he will have to intercept E at a closer point to T (provided P's speed is more than E's speed) thus increasing the possibility of E winning the game. If P continues to play sub-optimally , T falls out of his dominance region (refer Fig. 2.2). So pursuing I is the optimal play for P. Hence the optimal play for both the players is to head to the point $I(x_I, y_I)$ which is

closest to target T. In the rest of the thesis, by interception point we mean optimal interception point.

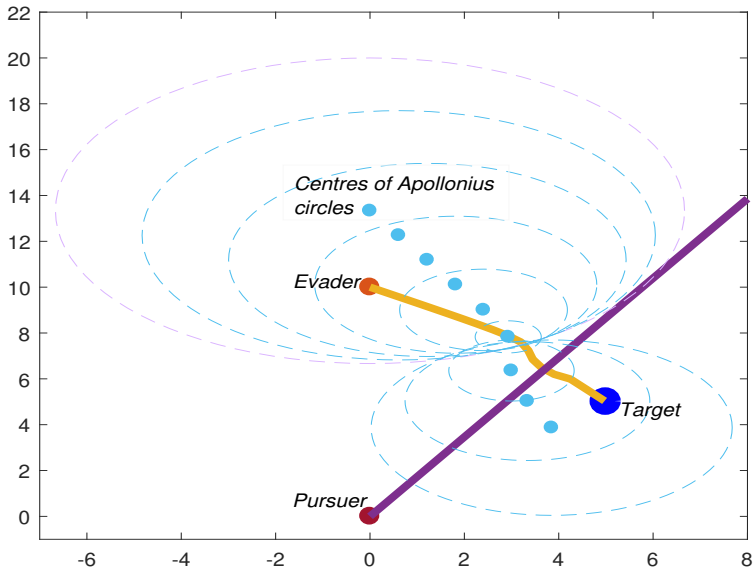

Figure 2.2: E plays optimally and P doesn't. Eventually E employs pure pursuit strategy when T falls in its dominance region

For P to head towards the optimal interception point, he has to have position and speed data of E. But the measurement is always associated with noise and no exact measurement in real time is possible. So if E's position and velocity are not known precisely, then P cannot know the exact point he has to head to, to intercept E. This work tries to find the heading angles of P at each instant in order to intercept E at nearest possible point to I. Analysis of the geometry of the game to get the essential insights necessary to attempt the solution is done in the following sections.

Let the positions of the P, T be (x_p, y_p), (x_T, y_T) respectively. Let the speed of the evader to the speed of the pursuer ratio, $\frac{v_e}{v_p} = k$ be a known quantity. For these given coordinates of P, T and speed ratio k, let the function $I_f(x, y, k) : \mathbb{R}^3 \rightarrow \mathbb{R}^2$ represents the interception point I when the evader is at (x, y). Let $I_f^*(x, y, k) : \mathbb{R}^3 \rightarrow \mathbb{R}^2$ represents the farthest point from T on the Apollonius circle C when the evader is at (x, y). These notations are maintained in the rest of the analysis presented in this thesis unless stated otherwise.

2.2 Possible evader locations for a given evader's speed which result in same interception point

Let the position of evader be (x_e, y_e). Let k be a known fixed quantity. Let $C_e\left(x_c, y_c\right)$ and R be center and radius of Apollonius circle C. The expressions for center C_e and radius R_e are (2.3) and (2.4) respectively. The objective is to find the set of all evader locations, $\mathscr{F}$ whose interception point is I. Note that T, I, and C_e lie on a straight line. For I to be the interception point corresponding to (x_e, y_e) i.e., $I_f(x_e, y_e, k) = I(x_I, y_I)$, it has to be the nearest point to T on C. In other words C_e must lie on the line joining T and I. Alternatively,

$$\frac{y_t - y_I}{x_t - x_I} = \frac{y_c - y_I}{x_c - x_I} = M. \tag{2.5}$$

Using the expressions (2.2) for x_c, y_c in (2.5) leads to

$$\frac{y_e - y_p k^2}{1 - k^2} - y_t = M\Big[\frac{x_e - x_p k^2}{1 - k^2} - x_t\Big], \tag{2.6}$$

which simplifies to

$$L:\ y_e - Mx_e = (y_t - Mx_t)(1 - k^2) = (y_I - Mx_I)(1 - k^2) \tag{2.7}$$

Thus all the evader points that belong to the set $\mathscr{F}$ must lie on the straight line L (2.7). However, the interception points of all points on L need not be I (refer Fig 2.3).

I has to lie on Apollonius circle of (x_e, y_e).

Therefore,

$$(x_I - x_c)^2 + (y_I - y_c)^2 = R^2 \tag{2.8}$$

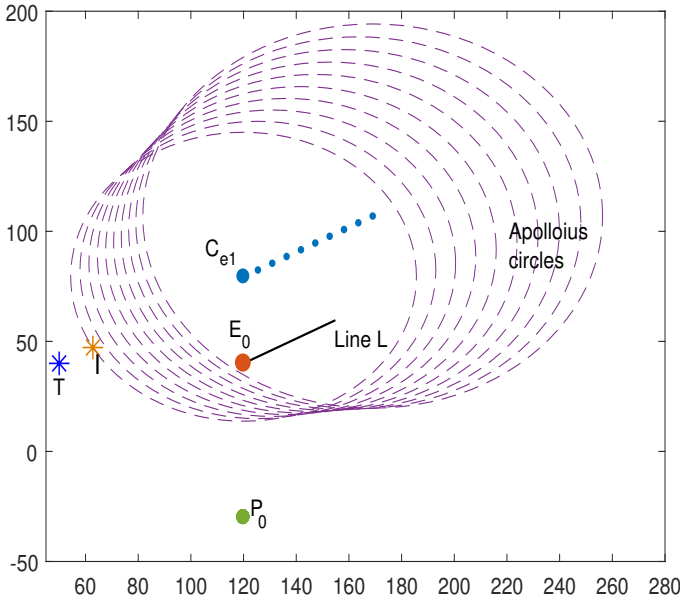

Figure 2.3: Apollonius circles of elements of set S_1

Substituting for x_c, y_c and R in (2.8) leads to

$$x_I^2 + y_I^2 - 2x_I x_c - 2y_I y_c = \frac{k^2(x_p^2 + y_p^2)}{1-k^2} - \frac{x_e^2 + y_e^2}{1-k^2}$$

Further simplification leads to the following circle equation

$$C_e : (x_e - x_I)^2 + (y_e - y_I)^2 = k^2((x_p - x_I)^2 + (y_p - y_I)^2) \tag{2.9}$$

So, elements of the set $\mathscr{F}$ i.e., all evader locations which result in same interception point satisfy (2.7) and (2.9).

As C_e is circle and L is a line, we get two solutions (except when L becomes tangent to C_e). Let the solution set be S . Out of these two solutions, one solution is always feasible. In-feasibility of the other solution depends on the location of T with respect to the centers of Apollonius circles corresponding to two solutions.

Two cases arise

- Target lying in between centers (refer Fig. 2.4). In this case one of the Apollonius circles encompasses target.

  Let the set of all solutions whose dominance regions do not contain target be S_f.

$$S_f = \{(x_e, y_e) \mid (x_e, y_e) \in S,\ T \notin R_E(x_e, y_e, k), I_f(x_e, y_e, k) = (x_I, y_I)\} \tag{2.10}$$

where $R_E(x_e, y_e, k)$ is the dominance region of evader when evader speed to pursuer speed ratio is k.

Let the set of all solutions whose dominance regions contain target be S_1.

$$S_1 = \{(x_e, y_e) \mid (x_e, y_e) \in S,\ T \in R_E(x_e, y_e, k),\ I_f(x_e, y_e, k) = (x_I, y_I)\} \quad (2.11)$$

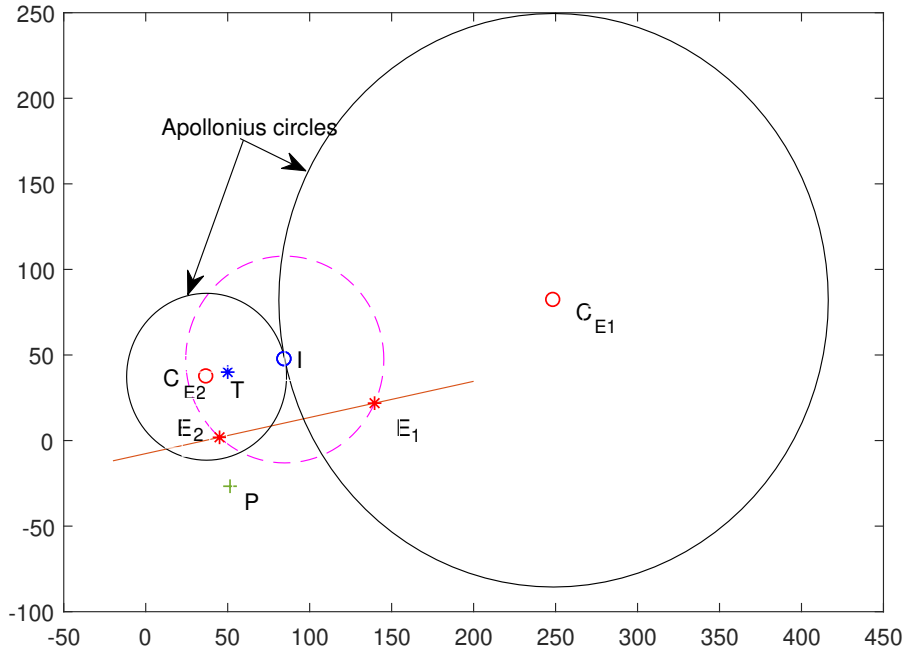

Figure 2.4: Case where interception point of (x_e, y_e) is (x_I, y_I), but as the Apollonius circle encircles T, pursuer has already lost the game if the actual evader position is E_2

- Target not lying in between centers (refer Fig. 2.5). In this case, I becomes the farthest point from target on the Apollonius circle corresponding to one of the solutions. Hence the solution for which $I_f^*(x_e, y_e, k) = (x_I, y_I)$ is infeasible.

  Let the set of all infeasible solutions be S_2

$$S_2 = \{(x_e, y_e) \mid (x_e, y_e) \in S,\ I_f^*(x_e, y_e, k) = (x_I, y_I)\} \quad (2.12)$$

So solutions set is $S_f \cup S_1 \cup S_2$. The number of elements in S is

$$n(S) = 2.$$

Let $x \in S - S_f$

$$n(S_1) = \begin{cases} 1 & if\ x \in S_1 \\ 0 & if\ x \notin S_1 \end{cases}$$

$$n(S_2) = \begin{cases} 1 & if\ x \in S_2 \\ 0 & if\ x \notin S_2 \end{cases}$$

Note $\mathscr{F} = S_f \cup S_1$ Hence when $n(S_1) = 1$, there are two evader points in $\mathbb{R}^2$ that result in same interception point, else only one point exists.

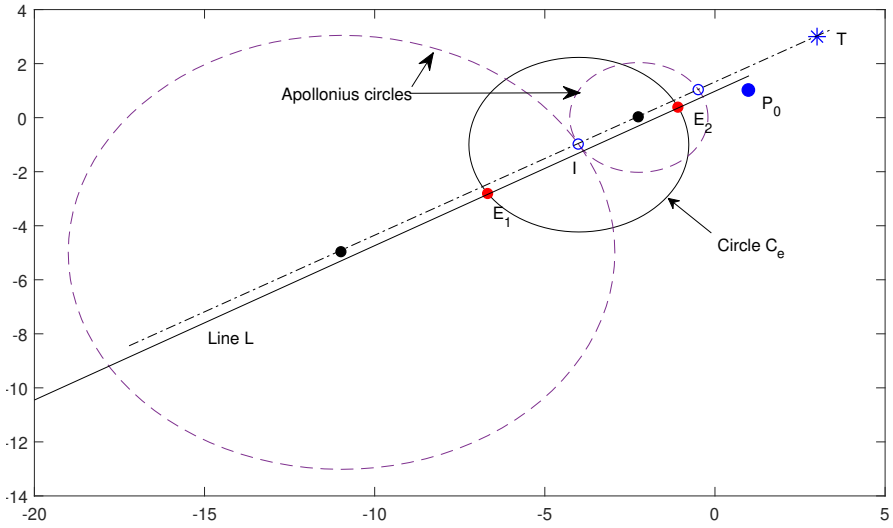

Figure 2.5: Infeasible case (x_e, y_e) whose corresponding interception point is not (x_I, y_I)

2.3 Possible evader locations which result in same interception point when evader's speed is also a variable

The objective is to find $\mathbb{F}$ set of all evader positions and their associated speeds which result in same interception point.

$$\mathbb{F} := \{(x_e, y_e, k) | I_f(x_e, y_e, k) = (x_I, y_I)\}$$

When speed of evader is also unknown, the equation (2.6) becomes

$$\left(\frac{y_e - y_p k^2}{1 - k^2}\right) - M\left(\frac{x_e - x_p k^2}{1 - k^2}\right) = y_t - M x_t \tag{2.13}$$

Simplifying, we get

$$(y_e - M x_e - c) = (y_p - M x_p - c) k^2 \tag{2.14}$$

where $c = y_t - M x_t$

The equation (2.9) remains the same.

$$C_e : (x_e - x_I)^2 + (y_e - y_I)^2 = k^2((x_p - x_I)^2 + (y_p - y_I)^2) \tag{2.15}$$

Eliminating k^2 from the equations (2.14) and (2.15),

$$(x_e - x_I)^2 + (y_e - y_I)^2 = \frac{y_e - Mx_e - c}{y_p - Mx_p - c}((x_p - x_I)^2 + (y_p - y_I)^2) \tag{2.16}$$

Simplifying, we get the following circle equation.

$$C_m : (x_e - x_{cm})^2 + (y_e - y_{cm})^2 = R_m^2 \tag{2.17}$$

Expressions for center (x_{cm}, y_{cm}) and radius R_m of circle C_m are given by (2.18), (2.19) respectively.

$$x_{cm} = x_I - \frac{HM}{2}, y_{cm} = y_I + \frac{H}{2} \tag{2.18}$$

$$R_m^2 = (x_I - x_{cm})^2 + (y_I - y_{cm})^2 = \frac{H^2(M^2 + 1)}{4} \tag{2.19}$$

where

$$H = \frac{(x_p - x_I)^2 + (y_p - y_I)^2}{(y_p - Mx_p - c)}$$

$$M = \frac{y_t - y_I}{x_t - x_I}$$

So set of all $\{(x_e, y_e), k\}$ which result in same interception point i.e., $I_f(x_e, y_e, k) = (x_I, y_I)$ satisfy (2.17), (2.20). Let the solution set be $\overline{S}$

$$k^2 = \frac{(x_e - x_I)^2 + (y_e - y_I)^2}{((x_p - x_I)^2 + (y_p - y_I)^2)} \tag{2.20}$$

We define the sets $\mathbb{S}_f, \mathbb{S}_1, \mathbb{S}_2$ following the definitions of S_f, S_1, S_2 from section (2.2). The set $\overline{S}$ is divided into these three sets to separate feasible solutions from infeasible solutions.

Let the set of all solutions of $\overline{S}$ whose dominance regions do not contain target be $\mathbb{S}_f$.

$$\mathbb{S}_f = \{(x_e, y_e, k) \mid (x_e, y_e, k) \in \overline{S},\ T \notin R_E(x_e, y_e, k), I_f(x_e, y_e, k) = (x_I, y_I)\} \tag{2.21}$$

Let the set of all solutions whose dominance regions contain target be $\mathbb{S}_1$.

$$\mathbb{S}_1 = \{(x_e, y_e, k) \mid (x_e, y_e, k) \in \overline{S},\ T \in R_E(x_e, y_e, k),\ I_f(x_e, y_e, k) = (x_I, y_I)\} \tag{2.22}$$

Let the set of all infeasible solutions be $\mathbb{S}_2$

$$\mathbb{S}_2 = \{(x_e, y_e, k) \mid (x_e, y_e, k) \in \overline{S},\ I_f^*(x_e, y_e, k) = (x_I, y_I)\} \tag{2.23}$$

From these definitions of the sets $\mathbb{S}_f, \mathbb{S}_1, \mathbb{S}_2$, it follows that $\mathbb{F} = \mathbb{S}_f \cup \mathbb{S}_1$. If true values of $(x_e, y_e, k) \in \mathbb{S}_1$, then pursuer loses the game as $T \notin R_p(x_e, y_e, k)$.

Assuming $\mathbb{S}_1, \mathbb{S}_2$ are non-empty sets,

$$\mathbb{S}_1 \cap \mathbb{S}_2 = \{(x_e, y_e, k) | I_f(x_e, y_e, k) = I_f^*(x_e, y_e, k) = (x_I, y_I)\} \tag{2.24}$$

This happens when center of Apollonius circle corresponding to (x_e, y_e), $(x_c, y_c) = (x_T, y_T)$.

2.4 Continuity of the function $I_f(x_e, y_e, k)$ over the sets $\mathbb{S}_f, \mathbb{S}_1, \mathbb{S}_2$

Let us parameterize the solution set $\overline{S}$ as follows.

$$x_e(\theta) = x_{cm} + R_m \cos\theta \tag{2.25}$$

$$y_e(\theta) = y_{cm} + R_m \sin\theta \tag{2.26}$$

$$k(\theta) = \frac{\sqrt{(x_I - (x_{cm} + R_m\cos\theta))^2 + (y_I - (y_{cm} + R_m\sin\theta))^2}}{\sqrt{(x_I - x_p)^2 + (y_I - y_p)^2}} \tag{2.27}$$

where x_{cm}, y_{cm}, R_m are given by (2.18), (2.19)

$x_e(\theta), y_e(\theta), k(\theta)$ are continuous functions of θ and center (x_c, y_c), radius R of circle C (given by (2.3), (2.4)) are continuous functions of x_e, y_e, k for $k < 1$. It follows that x_c, y_c, R are continuous functions of θ. The function $I_f(x_e, y_e, k)$ is given by (2.28)

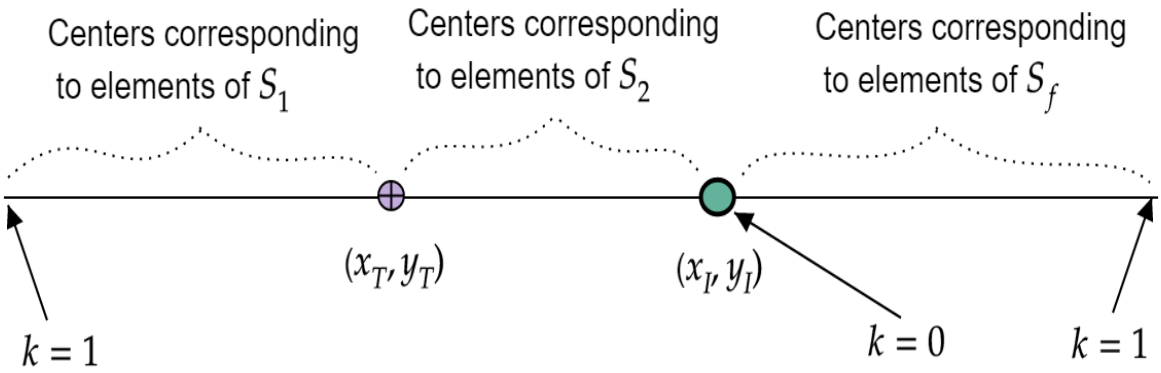

Figure 2.6: Centers of Apollonius circles of the elements of set $\overline{S}$ lie on a straight line

$$
\begin{aligned}
x_I &= \frac{x_e - x_p k^2}{1-k^2} \pm \sqrt{\frac{((x_e-x_p)^2+(y_e-y_p)^2)\frac{k^2}{(1-k^2)^2}}{1+(\frac{y_t(1-k^2)-y_e+y_p k^2}{x_t(1-k^2)-x_e+x_p k^2})^2}} \\
y_I &= \frac{y_e - y_p k^2}{1-k^2} \pm \sqrt{\frac{((x_e-x_p)^2+(y_e-y_p)^2)\frac{k^2}{(1-k^2)^2}}{1+(\frac{x_t(1-k^2)-x_e+x_p k^2}{y_t(1-k^2)-y_e+y_p k^2})^2}}
\end{aligned}
\tag{2.28}
$$

Note that $\pm$ in (2.28) is determined by the location of T.

Assuming $\mathbb{S}_1, \mathbb{S}_2$ are non-empty sets, it follows from their definitions that $I_f(x_e, y_e, k)$ is discontinuous at $\mathbb{S}_1 \cap \mathbb{S}_2$ where $'+'$ in (2.28) changes to $'-'$. Hence $I_f(x_e, y_e, k)$ is continuous function over the sets $\mathbb{S}_f, \mathbb{S}_1, \mathbb{S}_2$.

2.5 Some important results

Result I: *Pursuer coordinates (x_p, y_p) is one of the two solutions of (2.7), (2.9) when $k = 1$*

Proof:

When $k = 1$, (2.9) becomes

$$
(x_e - x_I)^2 + (y_e - y_I)^2 = (x_p - x_I)^2 + (y_p - y_I)^2 \tag{2.29}
$$

Pursuer coordinates (x_p, y_p) trivially satisfies (2.29). (x_p, y_p) also satisfies (2.7) (refer Fig. 2.7). This means when $k = 1$ one solution is always (x_p, y_p)

Define the function $D_e : \mathbb{R} \to \mathbb{R}$ as

$$
D_e(k) = \sqrt{(x_e - x_e^*)^2 + (y_e - y_e^*)^2}
$$

(x_e, y_e) and $(x_e^*, y_e^*) \in S$ for the given k and interception point (x_I, y_I). So $D_e(k)$ represents the distance between two elements of solution set S. Note that the line

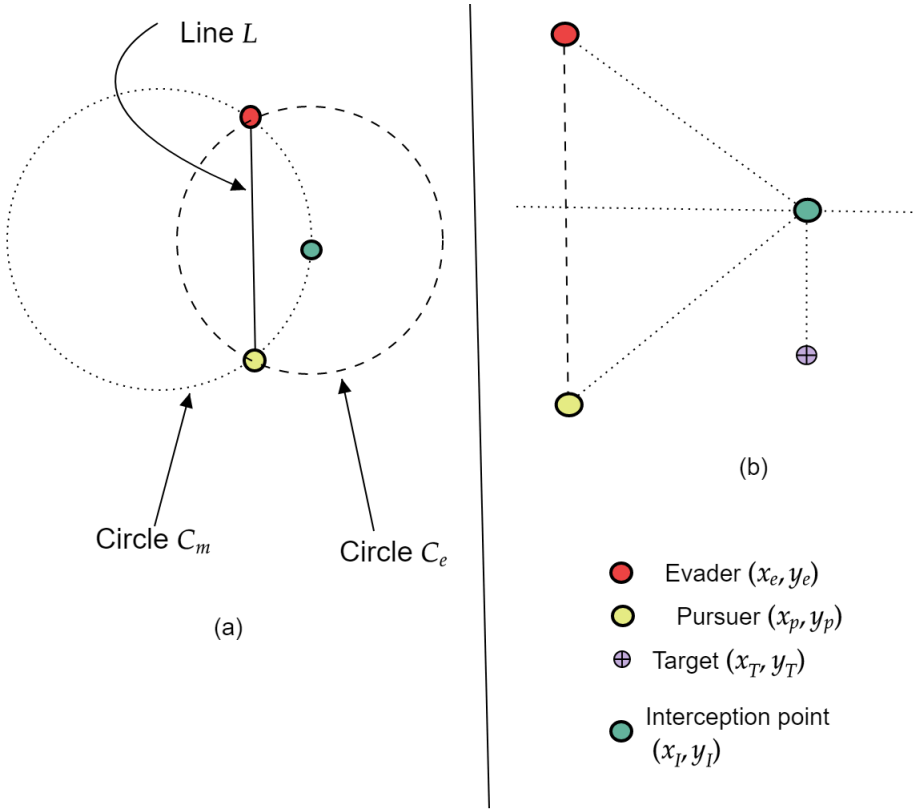

Figure 2.7: Topology of game when k=1. $\overline{EP} \parallel \overline{TI}$

joining the two elements of S forms a chord of circle C_m (2.17).

Define $\theta_{max}, \theta_{min}, \theta_{th}$ as

$$\theta_{max} = \arg\max_{\theta} k(\theta)$$

$$\theta_{min} = \arg\min_{\theta} k(\theta)$$

$$\theta_{th} = \frac{\theta_{min} + \theta_{max}}{2}$$

where $k(\theta)$ is given by (2.27)

Let $\theta_{min} < \theta_{th} < \theta_{max}$. $\theta_{max} - \theta_{min} = 180^0$. So, the line passing through $(x_e(\theta_{max}), y_e(\theta_{max})), (x_e(\theta_{min}), y_e(\theta_{min}))$, L_θ is a diameter of the circle C_m (2.17) and the slope of this line is $\frac{-1}{M}$ (refer Appendix B). The line L_θ is perpendicular to the line L (2.7).

It is to be noted that as $k(\theta)$ is a monotonically increasing function of θ when $\theta \in [\theta_{min}, \theta_{max}]$. As k increases from $k(\theta_{min})$ to $k(\theta_{th})$, $D_e(k(\theta))$ increases. $D_e(k(\theta_{th}))$ is equal to the diameter of circle C_m. As k increases from $k(\theta_{th})$ to $k(\theta_{max})$, $D_e(k(\theta))$

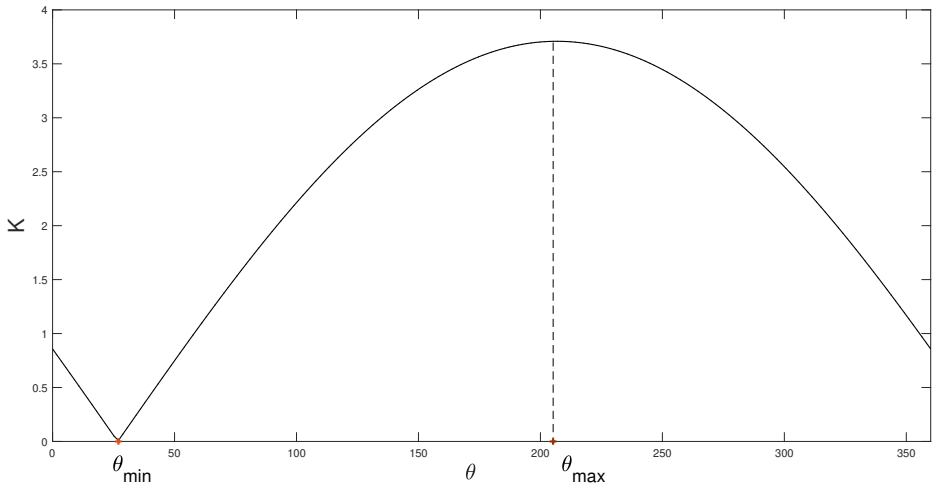

Figure 2.8: k vs θ

decreases.

Result II:

(a) If $k(\theta) \in [k(\theta_{th}), k(\theta_{max})]$ *and* $D_e(k(\theta)) = \mathscr{L}$*, then*

$$\sqrt{(x_p - x_e(\theta))^2 + (y_p - y_e(\theta))^2} < \mathscr{L} \tag{2.30}$$

(b) If $k(\theta) \in [k(\theta_{min}), k(\theta_{th})]$ *and* $D_e(k(\theta)) = \mathscr{L}$*, then*

$$\sqrt{(x_I - x_e(\theta))^2 + (y_I - y_e(\theta))^2)} < \mathscr{L} \tag{2.31}$$

where $\mathscr{L}$ is a positive constant and $k(\theta) < 1$.

Proof: *(a)* $(x_p, y_p) \in S$ when $k = 1 \Rightarrow (x_p, y_p, 1) \in \overline{S}$ (from *result I*).

As $\theta \in [\theta_{th}, \theta_{max}]$, $k(\theta) < 1$, $D_e(k(\theta)) < D_e(1)$.

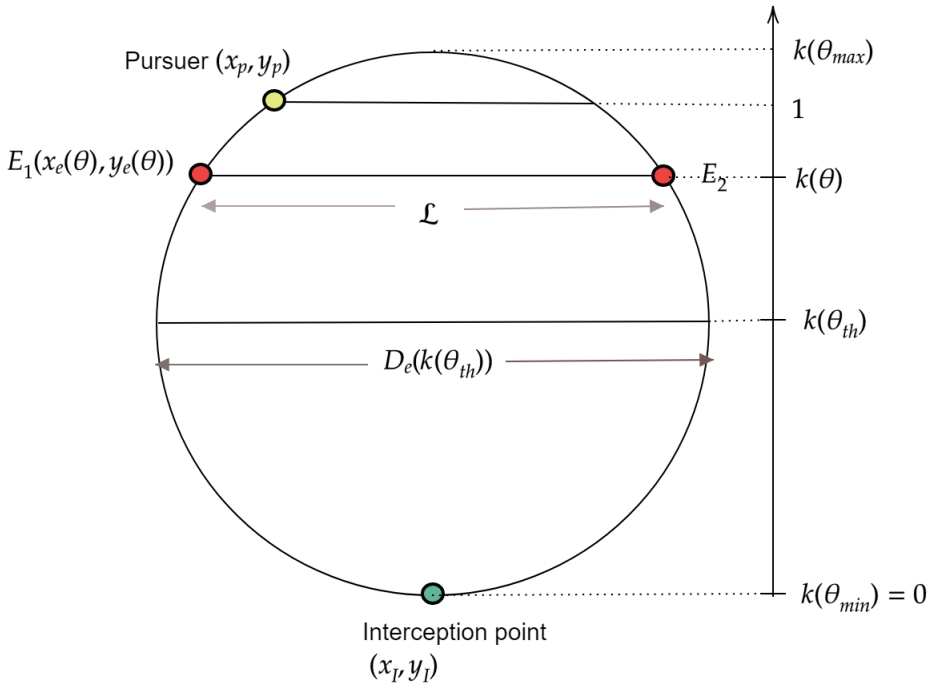

Figure 2.9: Relative positions of pursuer and evader on circle C_m when $k(\theta_{th}) < k < k(\theta_{max})$

Let $||\overset{\frown}{AB}||$ be length of arc $\overset{\frown}{AB}$. Note that length of chord $\overline{AB}$, $||\overline{AB}|| = ||\overset{\frown}{AB}||$.

$$||\overset{\frown}{E_1E_2}|| > ||\overset{\frown}{E_1P}||,$$

$$||\overset{\frown}{E_1E_2}|| > ||\overset{\frown}{E_2P}||$$

$$\Rightarrow ||\overline{E_1E_2}|| > ||\overline{E_1P}||,$$

$$||\overline{E_1E_2}|| > ||\overline{E_2P}||$$

(refer Fig. 2.9)

$$\sqrt{(x_p - x_e(\theta))^2 + (y_p - y_e(\theta))^2} < D_e(k(\theta))$$

$$\therefore \sqrt{(x_p - x_e(\theta))^2 + (y_p - y_e(\theta))^2} < \mathcal{L}$$

(b) $(x_I, y_I) \in S$ for $k(\theta_{min}) = 0$ as when $k = 0$, (2.27) becomes

$$(x_e - x_I)^2 + (y_e - y_I)^2 = 0 \tag{2.32}$$

$\Longrightarrow (x_I, y_I, 0) \in \overline{S}$

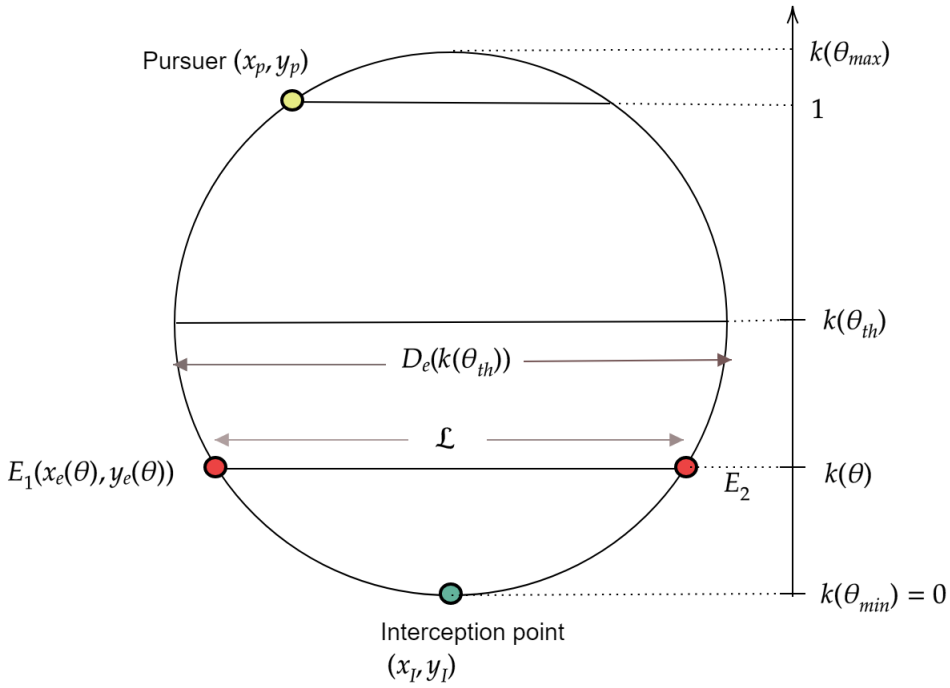

Figure 2.10: Relative positions of pursuer and evader on circle C_m when $k(\theta_{min}) < k < k(\theta_{th})$

$\theta \in [\theta_{min}, \theta_{th}]$, and $0 \leq k(\theta) < 1$

$$||\overset{\frown}{E_1E_2}|| > ||\overset{\frown}{E_1I}||,$$

$$||\overset{\frown}{E_1E_2}|| > ||\overset{\frown}{E_2I}||$$

$$\Rightarrow ||\overline{E_1E_2}|| > ||\overline{E_1I}||,$$

$$||\overline{E_1E_2}|| > ||\overline{E_2I}||$$

(refer Fig. 2.10)

$$\sqrt{(x_I - x_e(\theta))^2 + (y_I - y_e(\theta))^2} < D_e(k(\theta))$$

$$\therefore \sqrt{(x_I - x_e(\theta))^2 + (y_I - y_e(\theta))^2} < \mathcal{L}$$

CHAPTER 3

Game-theoretic analysis of Target Guarding Problem

3.1 Game formulation

Let target be at T. Let the closest point from T on the capture locus at time instant 'n' be I_n.

Let each of the players senses the position of other player for every ΔT time. Both the players are constrained to move on a straight line during this interval. The actions sets of players, S_p, S_e are given by (3.1).

$$S_i = \{\alpha_i | \alpha_i \in [0, 2\pi^c]\} \quad , \quad i = \{p, e\} \tag{3.1}$$

α_i is the heading angle of player i. Denote utility functions for pursuer and evader by U_p, U_e, defined in (3.2).

$$\begin{aligned} U_p(s_p, s_e) &= Dist(T, I_{n+1}) \\ U_e(s_e, s_p) &= -Dist(T, I_{n+1}) \end{aligned} \tag{3.2}$$

Given the positions of pursuer and evader at time instant 'n', the utility of pursuer is the distance between target and interception point at time instant '$n+1$'. As $U_p(s_p, s_e) + U_e(s_e, s_p) = 0, \forall s_e \in S_e, \forall s_p \in S_p$, TGP is a zero-sum game.

Let s_p^* and s_e^* denote the strategies of pursuer and evader when they pursue I_n. Rufus Isaacs in his pioneering work, argued that when pursuer employs s_p^*, there is always an incentive to deviate from any $s_e \neq s_e^*$. But the incentive to deviate from $s_e = s_e^*$ is zero. Same is the case for pursuer. If evader is playing optimally, any

strategy of pursuer, $s_p \neq s_p^*$ is strictly dominated by s_p^*. Mathematically,

$$\begin{aligned} U_p(s_p^*, s_e^*) > U_p(s_p, s_e^*) \quad \forall s_p \in S_p, \quad s_p \neq s_p^* \\ U_e(s_e^*, s_p^*) > U_e(s_e, s_p^*) \quad \forall s_e \in S_e, \quad s_e \neq s_e^* \end{aligned} \tag{3.3}$$

This implies,

$$\begin{aligned} BR_p(s_e^*) = s_p^* \\ BR_e(s_p^*) = s_e^* \end{aligned} \tag{3.4}$$

where $BR_i(s_j) = s_i, \;\; s_i \in S_i, \;\; i, j \in \{p, e\}, \;\; j \neq i,$

Thus (s_p^*, s_e^*) is the only pure strategy Nash equilibrium (PSNE) for this game.

Let the maxmin values of pursuer and evader be $\mathcal{V}_1, \mathcal{V}_2$ respectively.

Let a_p, b_e be set of all maxmin strategies of pursuer and evader respectively. The strategy pair set $\{(a, b) | a \in a_p, b \in b_e\}$ is defined as set of maxmin solutions.

The following theorem gives the relation between minmax, maxmin and Nash equilibrium strategies for a zero-sum game.

Von-Neumann Maxmin theorem: *A zero sum game has a PSNE if and only if* $\mathcal{V}_1 = \mathcal{V}_2$ *. In this case, the pure strategy Nash equilibria are exactly the maxmin solutions.*

We will understand this theorem in the present context. Given pursuer's strategy, evader tries to play in such a way that $Dist(T, I_{n+1}) \leq Dist(T, I_n)$, trying to minimize U_p and maximize U_e. Pursuer tries to maximize the minimum possible payoff.

$$\begin{aligned} a_p = \underset{s_p \in S_p}{\arg\max} \; \min_{s_e \in S_e} U_p(s_p, s_e) = \underset{s_p \in S_p}{\arg\min} \; \max_{s_e \in S_e} U_e(s_e, s_p) = s_p^* \\ U_p(a_p, s_e) = Dist(T, I_n) \geq U_p(s_p, s_e), \forall s_e \in S_e, \forall s_p \in S_p \end{aligned} \tag{3.5}$$

Similar argument holds for evader. Given evader's strategy, pursuer tries to play in

such a way that $Dist(T, I_{n+1}) \geq Dist(T, I_n)$, trying to minimize U_e and maximize U_p. In such a situation, evader's strategy must be equal to

$$\begin{gathered} a_e = \underset{s_e \in S_e}{\arg\max} \min_{s_p \in S_p} U_e(s_e, s_p) = \underset{s_e \in S_e}{\arg\min} \max_{s_p \in S_p} U_p(s_p, s_e) = s_e^* \\ U_e(a_e, s_p) = Dist(T, I_n) \geq U_e(s_e, s_p), \forall s_e \in S_e, \forall s_p \in S_p \end{gathered} \tag{3.6}$$

Hence $U_p(s_p^*, s_e^*) = U_e(s_e^*, s_p^*) = \mathcal{V}_1 = \mathcal{V}_2 = Dist(T, I_n)$.

As both players are rational and TGP is a simultaneous move game, we assume evader always plays the strategy s_e^* which is his minmax/maxmin strategy guaranteeing himself a minimum payoff of $-Dist(T, I_n)$. Note that s_e^* strictly dominates any $s_e \in S_e, s_e \neq s_e^*$ when pursuer plays s_p^* (3.3).

3.1.1 TGP in Bayesian game-theoretic framework

Let evader gets perfect measurements of position and speed of pursuer, while pursuer only gets perfect measurement of speed of evader and is ambiguous about the position of the evader. We will try to find the pure strategy Bayesian Nash equilibria (PSBNE) of this incomplete information Target Guarding Problem (TGP).

Type set of evader, $\Theta_e = \{E_1, E_2\}$. Type set of pursuer, $\Theta_p = \{P\}$.

The action sets available to players are

$$S_i = \left\{\alpha_i | \alpha_i \in [0, 2\pi^c]\right\} \quad , \quad i = \{p, (e1, e2)\} \tag{3.7}$$

The probability distribution over the evader type set be $\{x, y\}$, $x, y \geq 0$ and $x + y = 1$.

Let I_i, $(s_p^{(i)}, s_e^{(i)})$ be the interception point and PSNE when type of the evader is E_i, where $i = \{1, 2\}$.

The utility for pursuer at NE is

$$U_p(s_p^{(i)}, s_e^{(i)}) = Dist(T, I_i)$$

Denote the utility of the pursuer when type of evader is E_i and strategy of pursuer is α as $u_\alpha^{(i)}$.

Note that $s_p^{(i)}$ is the strictly dominant strategy for pursuer when type of the evader is E_i. So the following relation holds

$$\begin{aligned} u_\alpha^{(i)} &= U_p(s_p^{(i)}, s_e^{(i)}), \quad if \quad \alpha = s_p^{(i)} \\ &< U_p(s_p^{(i)}, s_e^{(i)}), \quad if \quad \alpha \neq s_p^{(i)} \end{aligned} \tag{3.8}$$

The game is represented in extensive form as shown in Figure 3.1

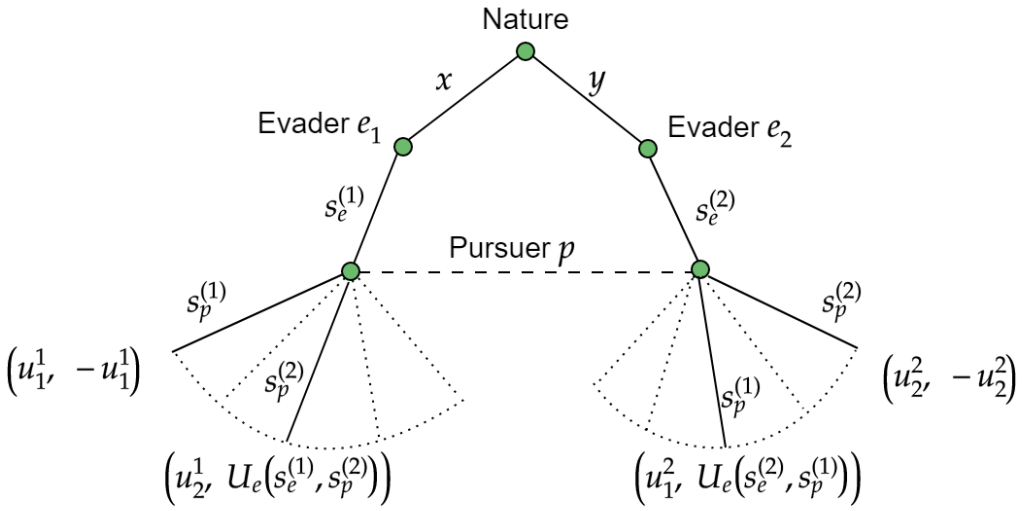

Figure 3.1: Extensive form representation of incomplete information TGP

The expected utility of pursuer as a function of α is given in (3.9).

$$\mathsf{E}_{E_i}\ U_p(\Theta_p, \Theta_e, \alpha, s_e^*(E_i)) = (x)\,u_\alpha^1 + (y)\,u_\alpha^2, \tag{3.9}$$

The Bayesian Nash equilibrium strategy of pursuer maximizes the expected utility (3.9). Hence, for a given probability distribution over the type set of evader, the

PSBNE strategy, α^* is given by (3.10)

$$\alpha^* = \underset{\alpha \in S_p}{\arg\max} \quad \mathsf{E}_{E_i}\ U_p(\Theta_p, \Theta_e, \alpha, s_e^*(E_i)) \tag{3.10}$$

where $s_e^*(E_i)$ is evader's NE strategy given evader is at E_i.

PSBNE of TGP is $(\alpha^*, s_e^{(1)}, s_e^{(2)})$.

3.1.2 Bayesian Nash equilibrium strategy of pursuer for larger type set of evader

Consider the following utility function for the pursuer

$$U_p(s_p, s_e) = \begin{cases} 1 & s_p = s_p^* \\ -1 & s_p \neq s_p^* \end{cases} \tag{3.11}$$

(3.4) still holds for this utility function. So (s_p^*, s_e^*) is PSNE.

The expected utility of pursuer as a function of α, given in (3.9) becomes

$$\mathsf{E}_{E_i}\ U_p(\Theta_p, \Theta_e, \alpha, s_e^*(E_i)) = \begin{cases} x - y & \alpha = s_p^{(1)} \\ y - x & \alpha = s_p^{(2)} \\ -1 & otherwise \end{cases} \tag{3.12}$$

Hence PSBNE is

$$\begin{cases} (s_p^{(1)}, s_e^{(1)}, s_e^{(2)}) & x > y \\ (s_p^{(2)}, s_e^{(1)}, s_e^{(2)}) & x < y \\ (s_p^{(1)} \sim s_p^{(2)}, s_e^{(1)}, s_e^{(2)}) & x = y \end{cases} \tag{3.13}$$

Let us extend the above analysis to the game with larger type set of evader. We are interested in finding the PSBNE in this case.

The type set of evader, $\Theta_e = \{E_1, E_2, ...E_N\}$.

Let the set of interception points corresponding to Θ_e be $\mathscr{I}$. For a given constant c_j, define the set L_{c_j} as

$$L_{c_j} = \{(x_I, y_I) | \frac{y_I - y_p}{x_I - x_p} = c_j, (x_I, y_I) \in \mathscr{I}\} \tag{3.14}$$

where $j = \{1, 2, 3...m\}$.

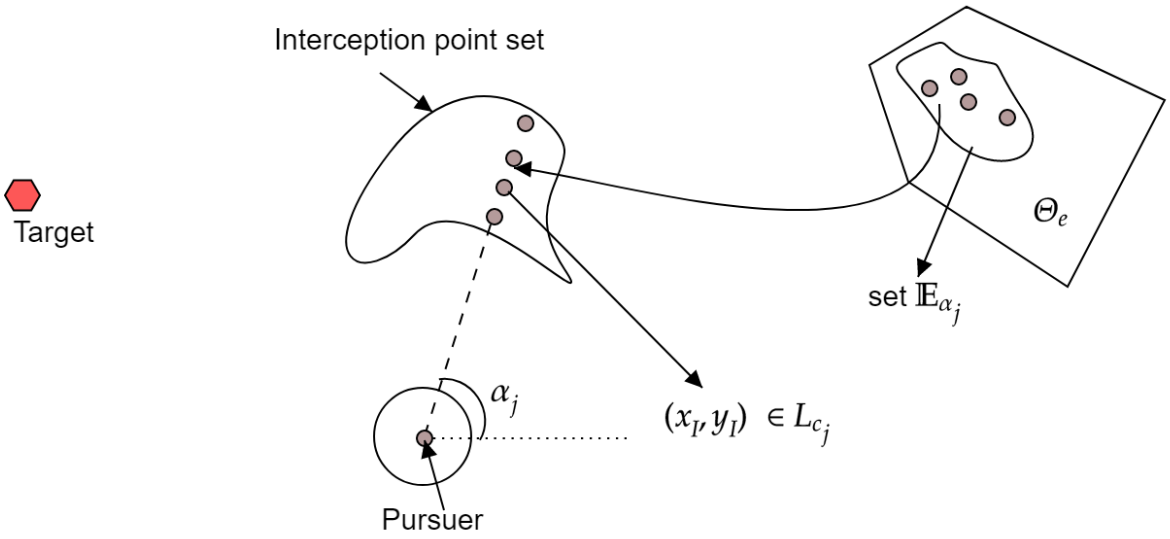

Figure 3.2: Set of all interception points which can be pursued with same heading angle have $U_p(s_p, s_e) = 1$

Let the set of all positions of evader in Θ_e which result in (x_I, y_I), $(x_I, y_I) \in L_{c_j}$ for a given c_j be $\mathbb{E}_{\alpha_j}$. Let $\mathbb{E}_{-\alpha_j} = \Theta_e - \mathbb{E}_{\alpha_j}$. Let number of elements in $\mathbb{E}_{\alpha_j}$ be n_j

The best response of each of evaders belonging to the set $\mathbb{E}_{\alpha_j}$ is to pursue interception point $(x_I, y_I) \in L_{c_j}$. Let $s(x_j^i)$ be the best response for $x_j^i \in \mathbb{E}_{\alpha_j}$, $i = \{1, 2, 3...n_j\}$, $j = \{1, 2, 3...m\}$

For evader positions belonging to set $\mathbb{E}_{\alpha_j}$, the best response of pursuer is to use the strategy $\alpha_j = \tan^{-1} c_j$.

The utilities of the pursuer given the strategies of evader are shown in above table.

$$\begin{aligned} U_p(\alpha_j, s(x_j^i)) &= 1 \\ U_p(\alpha_j, s(x_k^i)) &= -1 \end{aligned} \tag{3.15}$$

Evader

Pursuer

	x_1^1	x_1^2	x_1^3		$x_1^{n_1}$	$x_m^{n_m}$	x_2^1	$x_m^{n_m}$		$x_2^{n_2}$
α_1	1	1	1		1	−1	−1	−1		−1
α_2	−1	−1	−1		−1	−1	1	−1		1
α_m	−1	−1	−1		−1	1	−1	1		−1

Figure 3.3: Extensive form representation of incomplete information TGP

where $\alpha_j = BR(s(x_j^i))$, $k \neq j$, $k, j \in \{1,2,3...m\}$, $x_j^i \in \{x_j^1, x_j^2, x_j^3 ... x_j^{n_j}\}$

The expected utility of the pursuer when he employs the strategy α is

$$E_{E_i} U_p(\Theta_p, \Theta_e, \alpha_j, s_e^*(E_i)) = \sum_{i=1}^{n_j} F(x_j^i) U_p(\alpha_j, s(x_j^i)) + \sum_{\substack{l=1 \\ l \neq j}}^{m} \sum_{i=1}^{n_j} F(x_l^i) U_p(\alpha_j, s(x_l^i)) \tag{3.16}$$

where $F(x)$ is the probability distribution over the type set Θ_e. Substituting (3.15) in (3.16), (3.16) becomes

$$E_{E_i} U_p(\Theta_p, \Theta_p, \alpha_j, s_e^*(E_i)) = \sum_{i=1}^{n_j} F(x_j^i) - \sum_{\substack{l=1 \\ l \neq j}}^{m} \sum_{i=1}^{n_j} F(x_l^i) \tag{3.17}$$

Note that $\sum_{i=1}^{n_j} F(x_j^i)$ is the probability that pursuer's best response to $s(x_j^i)$ is heading angle α_j. Denote $\sum_{i=1}^{n_j} F(x_j^i)$ by $pr(\alpha_j)$.

Equation (3.16) becomes

$$E_{E_i} U_p(\Theta_p, \Theta_p, \alpha_j, s_e^*(E_i)) = pr(\alpha_j) - \sum_{\substack{l=1 \\ l \neq j}}^{m} pr(\alpha_l) \tag{3.18}$$

PSBNE strategy of pursuer, α^* satisfies the following inequalities.

$$E_{E_i}U_p(\Theta_p,\Theta_p,\alpha^*,s_e^*(E_i)) > E_{E_i}U_p(\Theta_p,\Theta_p,\alpha_j,s_e^*(E_i)), \quad \forall \alpha_j \neq \alpha^* \tag{3.19}$$

Solving inequalities of (3.19), we get

$$pr(\alpha^*) > pr(\alpha_j), \quad \forall \alpha_j \neq \alpha^* \tag{3.20}$$

Hence PSBNE for incomplete information TGP is given by $(\alpha^*, (s_e^*(E_1), s_e^*(E_2), ...s_e^*(E_N)))$, where α^* is most probable heading angle.

Let us find the PSBNE of the TGP with (3.2) as the utility function of the pursuer. Before we proceed, we have to partition the set $\mathbb{E}_{\alpha_j}$ as follows

$$\begin{gathered} E_{\alpha_j}^{I_k} = \{y_j^i(k) | I_f(y_j^i(k)) = I_j^k\}, \quad i \in \{1,2,3....N_j^k\}, \quad k \in \{1,2,3.....q_j\} \\ \bigcup_{k=1}^{q_j} E_{\alpha_j}^{I_k} = E_{\alpha_j} \\ \bigcup_{j=1}^{m} E_{\alpha_j} = \Theta_e \end{gathered} \tag{3.21}$$

where $I_f(y_j^i(k)) = I_j^k$ is the interception point when evader is at $y_j^i(k)$, $i \in \{1,2,3....N_j^k\}$.

$E_{\alpha_j}^{I_k}$ is set of all evader positions whose interception point is I_j^k, $I_j^k \in L_{c_j}$. Let the best response of the evader at $y_j^i(k)$ be $s(y_j^i(k))$. The payoff for the pursuer when his strategy is $BR(s(y_j^i(k)))$, is

$$U_p(\alpha_j, s(y_j^i(k))) = Dist(T, I_j^k) \tag{3.22}$$

When evader is at $y_j^i(k)$ and his strategy is $s(y_j^i(k))$, α_l, $l \neq j$ is sub-optimal strategy

of pursuer. Then pursuer's payoff is $U_p(\alpha_j, s(y_l^i(k))) \neq Dist(T, I_l^k),\ k \in \{1,2,3....q_j\}$.

$$E_{E_i}U_p(\Theta_p,\Theta_p,\alpha_j,s_e^*(E_i)) = \sum_{i=1}^{n_j} F(x_j^i)U_p(\alpha_j,s(x_j^i)) + \sum_{\substack{l=1\\l\neq j}}^{m}\sum_{i=1}^{n_j} F(x_l^i)U_p(\alpha_j,s(x_l^i))$$
$$= \sum_{k=1}^{q_j}\sum_{i=1}^{N_k^j} F(y_j^i(k))U_p(\alpha_j,s(y_j^i(k))) + \sum_{\substack{l=1\\l\neq j}}^{m}\sum_{k=1}^{q_j}\sum_{i=1}^{N_k^l} F(y_l^i(k))U_p(\alpha_j,s(y_l^i(k))) \tag{3.23}$$

Note that $\sum_{i=1}^{N_k^j} F(y_j^i(k))$ is sum of probabilities of all evaders being at $y_j^i(k)$. By our notation, all these evader positions result in same interception point I_j^k. So $\sum_{i=1}^{N_k^j} F(y_j^i(k))$ is equal to the probability of interception point being at I_j^k. Represent the probability of interception point being at I_j^k as $pr(I_j^k)$. Equation (3.23) becomes

$$E_{E_i}U_p(\Theta_p,\Theta_p,\alpha_j,s_e^*(E_i)) = \sum_{k=1}^{q_j} pr(I_j^k)U_p(\alpha_j,s(y_j^i(k))) + \sum_{\substack{l=1\\l\neq j}}^{m}\sum_{k=1}^{q_j} pr(I_l^k)U_p(\alpha_j,s(y_l^i(k))) \tag{3.24}$$

Substitution of (3.22) in (3.24) results in

$$E_{E_i}U_p(\Theta_p,\Theta_e,\alpha_j,s_e^*(E_i)) = \sum_{k=1}^{q_j} pr(I_j^k)Dist(T,I_j^k) + \sum_{\substack{l=1\\l\neq j}}^{m}\sum_{k=1}^{q_j} pr(I_l^k)U_p(\alpha_j,s(y_l^i(k))) \tag{3.25}$$

The PSBNE strategy of the pursuer α^* is the strategy that maximizes expected utility (3.25).

$$\alpha^* = \underset{\alpha_j\in S_p}{\arg\max}\, E_{E_i}U_p(\Theta_p,\Theta_e,\alpha_j,s_e^*(E_i)) \tag{3.26}$$

where S_p is the action set of pursuer given in (3.1).

Hence PSBNE of TGP is $(\alpha^*, (s_e^*(E_1), s_e^*(E_2), s_e^*(E_3).....s_e^*(E_N)))$.

CHAPTER 4

Kalman filter for TGP

4.1 A brief introduction

Kalman filtering is a clever technique to filter the noise present in the measurements of states using the dynamical model of the system and Bayesian updating. The estimation algorithm is a two step process. In the first step, it estimates the current state variables and their uncertainties using the state space model of the system. In the second step, it finds the posterior probability distributions of the states given prior probability distributions, using the noise corrupted measurements and corrects the estimates of mean values of the states. Kalman filter is a recursive linear unbiased estimator and gives optimal results for linear systems when process noises and measurement noises are independent, mean zero Gaussian random variables.

For non-linear systems, extensions of Kalman filtering algorithm have been developed. One such extension is extended Kalman filter (EKF) which linearizes the system at the current estimates of the states and given inputs. As we will see that the dynamical system governing the evader's kinematics is a non-linear system, we employ EKF algorithm to obtain better estimates of evader's position and speed. Other extensions include Unscented Kalman filter (UKF) and particle filters. UKF calculates linearized approximation of the states based on linearization values of function at selected points. Particle filters are nonparametric implementations of Bayes filters (unlike Kalman filter which estimates only the mean and variance of the random variables with linear dynamics) and correct the estimates based on the measurements. Instead of representing the distribution by a parametric form, particle filters represent a distribution by set of samples drawn from this distribution. These filters are

well-suited for non-linear systems because of their efficient algorithms, but are computationally intensive. As a first step in designing an estimator to address the filtering problem, we design EKF and analyse its performance.

4.1.1 EKF algorithm

Consider the system with model

$$\begin{aligned} x_k &= f(x_{k-1}, u_k) + v_k \\ z_k &= h(x_k) + w_k \end{aligned} \tag{4.1}$$

u, z are input and output of the system. v_k, w_k are mean zero independent Gaussian distributed process noise and measurement noise. Let the process error covariance matrix be Q and measurement error covariance matrix be R. If the model perfectly describes the system, Q is zero. Q usually models the modeling, linearization and discretization errors. Matrix Q is usually treated as the tuning parameter and is used to exact best performance from Extended Kalman filter.

Kalman observer model:

$$\hat{x}_{k|k-1} = f(\hat{x}_{k-1|k-1}, u_k) \tag{4.2}$$

Linearization of model and output is done at current estimates and applied input.

$$\begin{aligned} A_n &= \frac{\partial f}{\partial x}\Big|_{\hat{x}_{k-1|k-1}, u_k} \\ C_n &= \frac{\partial h}{\partial x}\Big|_{\hat{x}_{k|k-1}} \end{aligned} \tag{4.3}$$

If initial state estimates are not available, they can be back calculated from output if no. of outputs and no. of states are equal. The initial P matrix,$P_{0|0}$ reflects how close the initial estimates of states are to the actual state values. P matrix conveys to

the Kalman observer how important are the initial estimates in estimating the state variables and so is initialized accordingly.

To design an observer, the system must be observable. A system is said to be locally weakly observable if the observability matrix O_n, of the pair A_n, C_n is non-singular. The full-rank condition on O_n is only sufficient to declare that system is locally weakly observable. If in case O_n is rank-deficient, EKF can only estimate states which are observable.

Algorithm 1 Kalman filter iteration process

Initialization:
$\hat{X}_{0|0} = h^{-1} Z_0$,
loop:
Prediction:
$\hat{X}_{n|n-1} = f(\hat{X}_{n-1|n-1}, u_n)$
$P_{n|n-1} = A_n P_{n-1|n-1} A_n^T + Q$
Correction:
Measurement residual: $\tilde{y}_n = Z_n - h(\hat{X}_{n|n-1})$
Near-optimal Kalman gain: $\hat{K}_n = P_{n|n-1} C^T (C P_{n|n-1} C^T + R)^{-1}$
$\hat{X}_{n|n} = \hat{X}_{n|n-1} + K_n \tilde{y}_n$
$P_{n|n} = (I - K_n C^T) P_{n|n-1}$
goto *loop*.
close;

The algorithm of EKF is shown in Alg. 1. The computational ease of the Kalman filter is because of the brevity of its algorithm which allows for its use in many real world estimation problems.

4.2 Extended Kalman Filter with evader coordinates and k as states

Pursuer and evader move in a straight line toward the interception point which remains stationary if both players play optimally. As pursuer doesn't have accurate data to calculate (x_{I_n}, y_{I_n}) his path will be suboptimal. Every instant evader senses the current location of pursuer and moves toward instantaneous interception point.

The difference equations governing evader's kinematics are

$$x_{e_{n+1}} = x_{e_n} + (k_n V_p \Delta T)\cos\theta_{e_n} + \eta \tag{4.4}$$

$$y_{e_{n+1}} = y_{e_n} + (k_n V_p \Delta T)\sin\theta_{e_n} + \alpha \tag{4.5}$$

$$k_{n+1} = k_n + \beta \tag{4.6}$$

$$\theta_p = tan^{-1}\left(\frac{y_{I_n} - y_{p_n}}{x_{I_n} - x_{p_n}}\right)$$

$$\theta_e = tan^{-1}\left(\frac{y_{I_n} - y_{e_n}}{x_{I_n} - x_{e_n}}\right)$$

where $k = \frac{V_e}{V_p}$. Input to the system, (x_{p_n}, y_{p_n}) is the position of the pursuer. θ_{e_n} is heading angle of evader and (x_{I_n}, y_{I_n}) is interception point pursued by evader at time instant 'n'. The expressions for x_{I_n}, y_{I_n} can be obtained by solving the line passing through target, (x_T, y_T) and center of Apollonius circle (x_c, y_c) (4.7), and Apollonius circle (2.2).

$$y - y_T = M(x - x_T) \tag{4.7}$$

$$x_{I_n} = x_{c_n} + sgn(x_T - x_{c_n})\sqrt{\frac{\frac{k_n^2}{(1-k_n^2)^2}((x_{e_n} - x_{p_n})^2 + (y_{e_n} - y_{p_n})^2)}{1 + M^2}} \tag{4.8}$$

$$y_{I_n} = y_T + M(x_{I_n} - x_T) \tag{4.9}$$

$sgn(x_T - x_{c_n})$, sign function, distinguishes between closest point and farthest point of the two solutions depending on the relative position of x_{c_n} with respect to x_T

$$x_{c_n} = \frac{x_{e_n} - x_{p_n}k_n^2}{1 - k_n^2}$$

$$y_{c_n} = \frac{y_{e_n} - y_{p_n}k_n^2}{1 - k_n^2}$$

$$M = \frac{y_T - y_{c_n}}{x_T - x_{c_n}}$$

η, α, β are assumed to be white noise with process error covariance matrix Q to account for discretization errors. As the speed ratio is constant, we could let β to be zero.But considering β with very small value of variance, gives us the flexibility to

tune Q matrix in order to improve the performance of EKF [7]. There's no input noise as the input to the system, pursuer's coordinates, is known to both evader and pursuer.

Output

Pursuer measures evader's location (x_e, y_e) and speed ratio [1] k inaccurately.

So, the output is

$$Z_n = CX_n + \begin{pmatrix} \eta_m \\ \alpha_m \\ \beta_m \end{pmatrix}$$

where

$$X_n = \begin{pmatrix} x_{e_n} \\ y_{e_n} \\ k_{e_n} \end{pmatrix}$$

C is identity matrix of order 3. $\eta_m, \alpha_m, \beta_m$ are assumed to be i.i.d noise with measurement error covariance matrix R.

$$R = \begin{pmatrix} \sigma_x^2 & 0 & 0 \\ 0 & \sigma_y^2 & 0 \\ 0 & 0 & \sigma_k^2 \end{pmatrix} \tag{4.10}$$

Kalman observer model

$$G := \hat{x}_{e_{n+1|n}} = \hat{x}_{e_{n|n}} + (\hat{k}_{e_{n|n}} V_p \Delta T) \cos\hat{\theta}_{e_n} \tag{4.11}$$

[1] Pursuer measures speed of evader. As speed ratio, $k = \frac{v_e}{v_p}$ is one of the states and all the expressions we have been using depend on k, it is convenient to assume that pursuer measures speed ratio.

$$H := \hat{y}_{e_{n+1|n}} = \hat{y}_{e_{n|n}} + (\hat{k}_{e_{n|n}} V_p \Delta T) \sin\hat{\theta}_{e_n} \tag{4.12}$$

$$L := \hat{k}_{n+1|n} = \hat{k}_{n|n} \tag{4.13}$$

where

$$\hat{\theta}_{e_n} = \tan^{-1}\left(\frac{\hat{y}_{e_{n|n}} - \hat{y}_{I_n}}{\hat{x}_{e_{n|n}} - \hat{x}_{I_n}}\right)$$

$$\hat{x}_{I_n} = \frac{\hat{x}_{e_{n|n}} - x_{p_n}\hat{k}_n^2}{1-\hat{k}_n^2} \pm \sqrt{\frac{\frac{\hat{k}_n^2}{(1-\hat{k}_n^2)^2}((\hat{x}_{e_{n|n}} - x_{p_n})^2 + (\hat{y}_{e_{n|n}} - y_{p_n})^2)}{1+\hat{M}^2}}, \tag{4.14}$$

$$\hat{y}_{I_n} = y_T + \hat{M}(\hat{x}_{I_n} - x_T) \tag{4.15}$$

$$\hat{M} = \frac{y_T(1-\hat{k}_n^2) - (\hat{y}_{e_{n|n}} - y_{p_n}\hat{k}_n^2)}{x_T(1-\hat{k}_n^2) - (\hat{x}_{e_{n|n}} - x_{p_n}\hat{k}_n^2)} \tag{4.16}$$

Prediction error covariance matrix, $P_{n+1|n} = A_n P_{n|n} A_n^T + Q$

where

$$A_n = \begin{pmatrix} \frac{\partial G}{\partial x_e} & \frac{\partial G}{\partial y_e} & \frac{\partial G}{\partial k_e} \\ \frac{\partial H}{\partial x_e} & \frac{\partial H}{\partial y_e} & \frac{\partial H}{\partial k_e} \\ \frac{\partial V}{\partial x_e} & \frac{\partial V}{\partial y_e} & \frac{\partial V}{\partial k_e} \end{pmatrix} = \begin{pmatrix} \frac{\partial G}{\partial x_e} & \frac{\partial G}{\partial y_e} & \frac{\partial G}{\partial k_e} \\ \frac{\partial H}{\partial x_e} & \frac{\partial H}{\partial y_e} & \frac{\partial H}{\partial k_e} \\ 0 & 0 & 1 \end{pmatrix}_{(\hat{x}_{e_{n|n}}, \hat{y}_{e_{n|n}}, \hat{k}_{e_{n|n}}, x_{p_n}, y_{p_n})} \tag{4.17}$$

The linearization operation is performed after substituting (4.8), (4.9) in (4.4) and (4.5).

4.2.1 Condition to check if evader has won the game

We are interested in finding the set of all evader locations for a constant evader speed, V which result in same interception point.

For target to be the interception point, it has to satisfy the equation of Apollonius

circle (2.2). So (4.18) follows.

$$(x_T - x_c)^2 + (y_T - y_c)^2 = R_c^2 \tag{4.18}$$

Substituting expressions for center and radius of Apollonius circle, we get the following the circle equation.

$$(x_e - x_T)^2 + (y_e - y_T)^2 = k^2((x_{p_n} - x_T)^2 + (y_{p_n} - y_T)^2) \tag{4.19}$$

where k is ratio of speeds of evader and pursuer. Denote the radius of the circle by R_{T_n}.

So the locus of all evader positions (x_e, y_e) for which target is the interception point is a circle with center (x_T, y_T). So if distance between target and evader is smaller than R_{T_n} then target will be in the dominance region of evader.

Kalman filter produces the estimates of mean and state error covariance values of x_e, y_e, V. Using the estimated speed of evader, V, the set of all evader positions whose interception point is target can be found. Denote the circle by $C_{\hat{V}}$

Consider a rectangle $\mathscr{R}$ with length and breadth equal to $6\hat{\sigma}_x, 6\hat{\sigma}_y$. Let the center of this rectangle be at $\hat{x}_{e_{n|n}}, \hat{y}_{e_{n|n}}$ (refer 4.18).

The following condition is used to check if target is in evader's dominance region

$$\sqrt{(3\hat{\sigma}_x)^2 + (3\hat{\sigma}_y)^2} + R_{T_n} \leq \sqrt{(x_T - \hat{x}_{e_{n|n}})^2 + (y_T - \hat{y}_{e_{n|n}})^2} \tag{4.20}$$

This condition means that if $\mathscr{R}$ and $C_{\hat{V}}$ intersect, then there is non-zero probability that pursuer has lost the game. As the game progresses, $\hat{\sigma}_x, \hat{\sigma}_y$ converge to zero and estimates of to the actual speed of evader, we can check this condition to find if evader has won the game. Evader wins the game if $\mathscr{R}$ is inside $C_{\hat{V}}$.

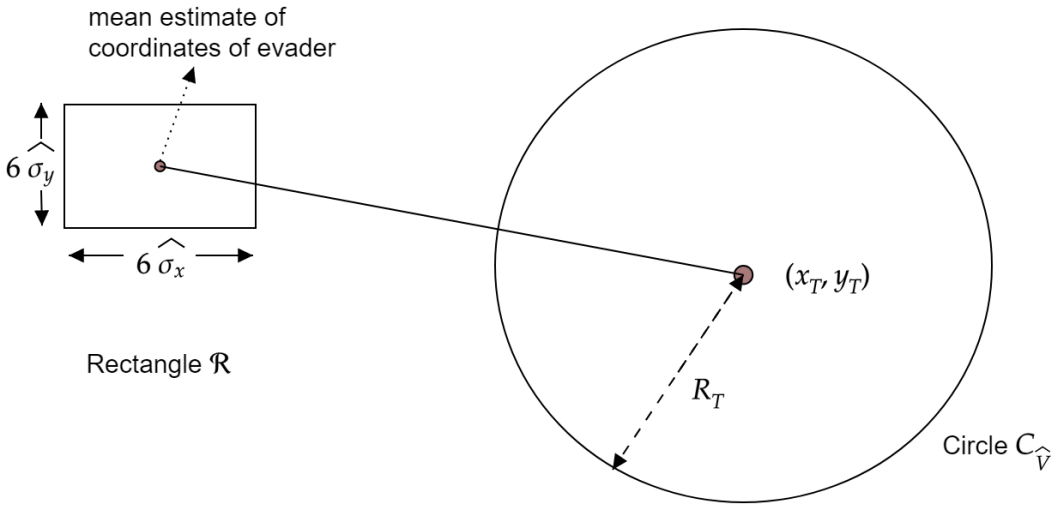

Figure 4.1: If evader is inside the circle $C_{\hat{V}}$ then target is in evader's dominance region

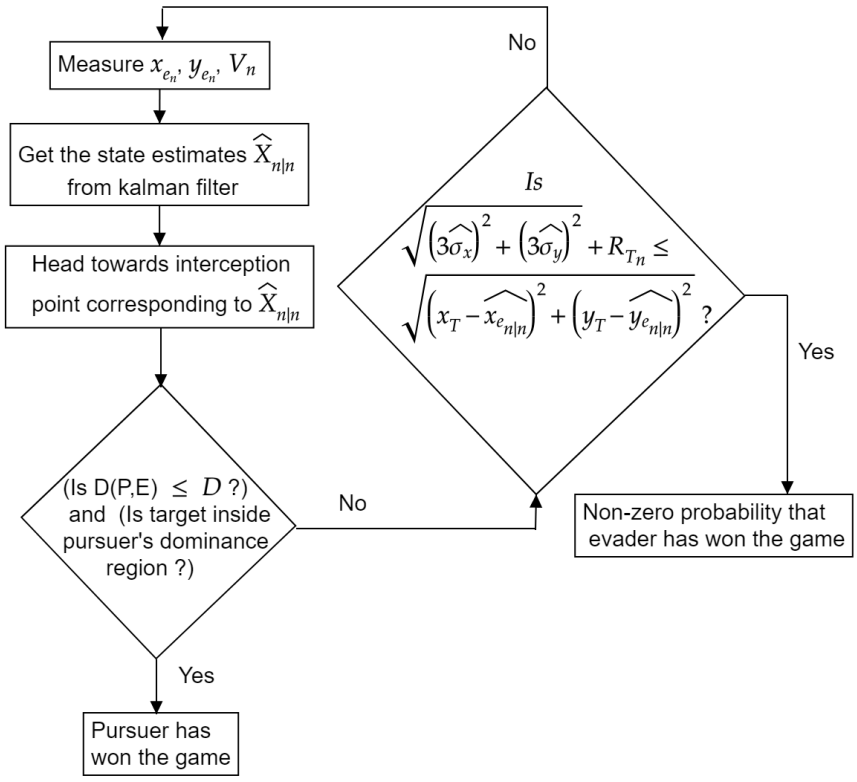

Figure 4.2: Flowchart showing the decision making algorithm of pursuer

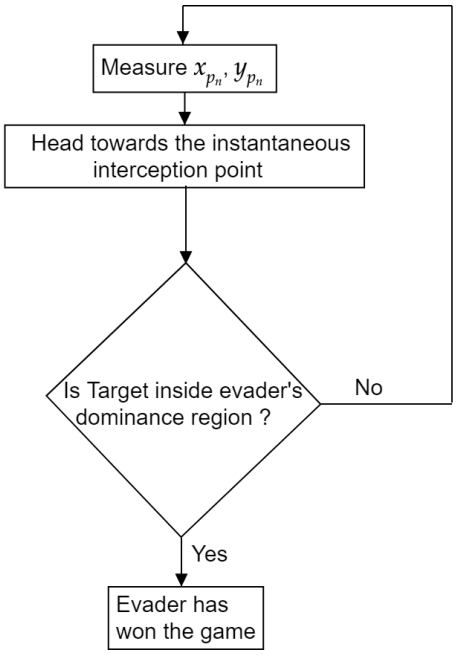

Figure 4.3: Flowchart showing the decision making algorithm of evader

4.2.2 Simulation results:

As the system is non-linear, it is through simulations alone, the performance of the Kalman observer can be analysed. Also as the location of target is independent of pursuer's location, pursuer may fail to protect the target because of his sub-optimal play if he is not close to the target. Simulation study will help put approximate bounds on the distance of evader to the target at the beginning of the game for given positions of pursuer and target considering the sub-optimal play of pursuer.

Simulation results are presented for two different sets of measurement and process noise variance values. The measure of optimality of pursuer's path when measurements are corrupted by noise is the distance between target and interception point when pursuer reaches within specified distance D from the evader.

Auto-covariances of states x_e, y_e reached non-zero steady state values approximately after $n = 7$. This implies Kalman filter was not able to improve the estimates of these states using measurements after $n = 7$ (refer 4.6a and 4.6b). However, the auto-covariance of the state k settled only after $n = 15$ which means Kalman filter improved its estimate of k using measurements until $n = 15$ and so the estimate of k

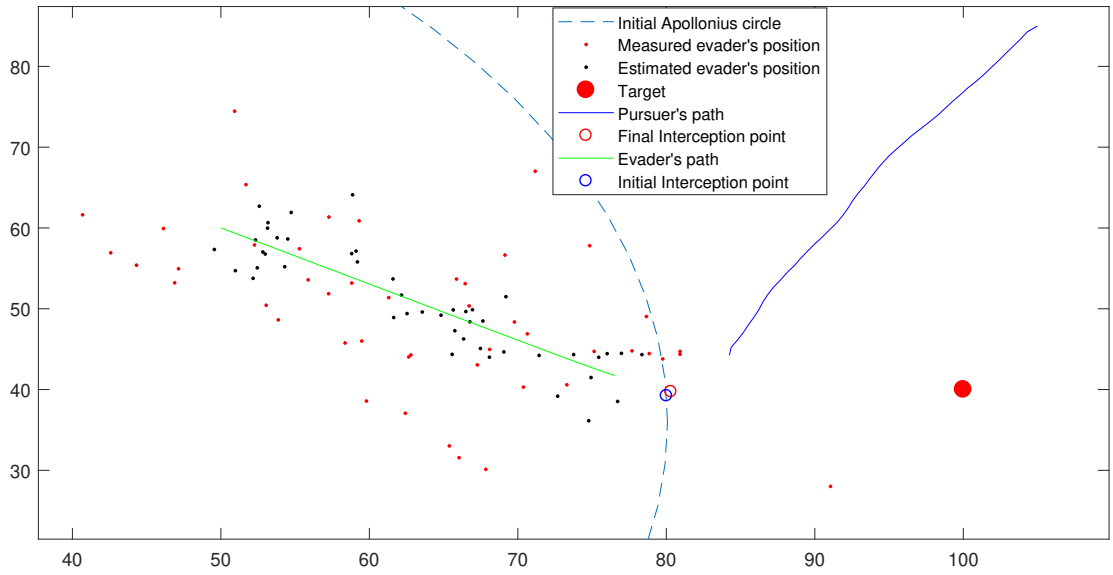

(a) Plot with noise variance $\sigma_x^2, \sigma_y^2, \sigma_k^2$

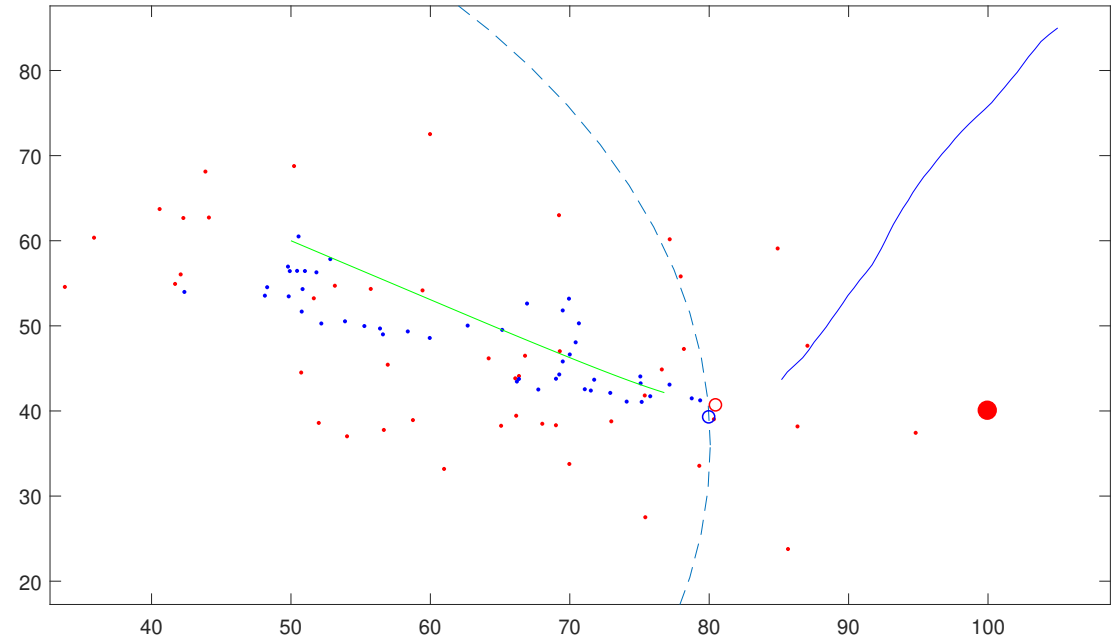

(b) Plot with noise variance $3\sigma_x^2, 3\sigma_y^2, 3\sigma_k^2$

Figure 4.4: Pursuer won in both cases as he reached within a pre-specified distance from evader. Distance between target and final interception point is approximately equal to the distance between target and initial interception point

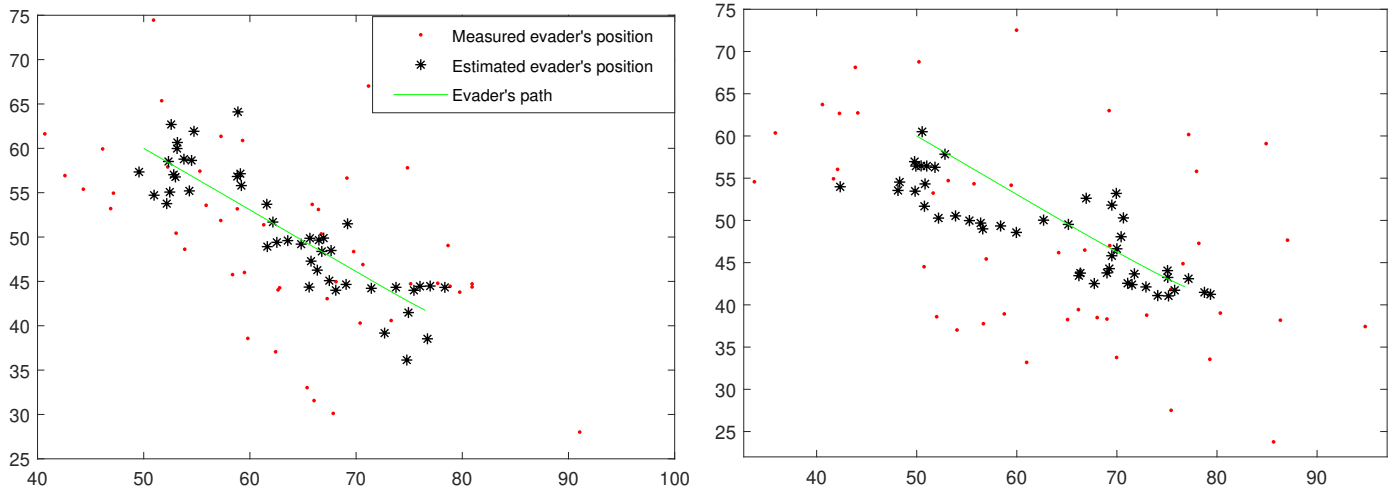

(a) Plot with noise variance $\sigma_x^2, \sigma_y^2, \sigma_k^2$

(b) Plot with noise variance $3\sigma_x^2, 3\sigma_y^2, 3\sigma_k^2$

Figure 4.5: Estimates of position of evader doesn't converge onto the true position because of non-zero process noise.

converged to true value in both cases 4.5a, 4.5b.

Paths followed by pursuer and evader are shown in figures 4.3a and 4.3b. Estimates of evaders position during the game given by the Kalman filter for both the values of variances are shown in figures 4.4a and 4.4b.Estimates of position of evader doesn't converge onto the true position as the simulations are run with non-zero process noise. If process noise is zero, the error between true position and estimate of evader's position converges to zero. Note that process noise is assumed in order to account for the manueverability limitations of the evader.

Plot 4.7 presents a game where target is close to initial interception point. By the time pursuer is within D units distance from evader, target is in evader's dominance region. Evader wins the game. This is because pursuer's initial position is far from the target and so pursuer, owing to his sub-optimal play, couldn't get enough time to protect the target. When measurement data is associated with noise, pursuer wins the game only if he is close to the target at the beginning of the game.

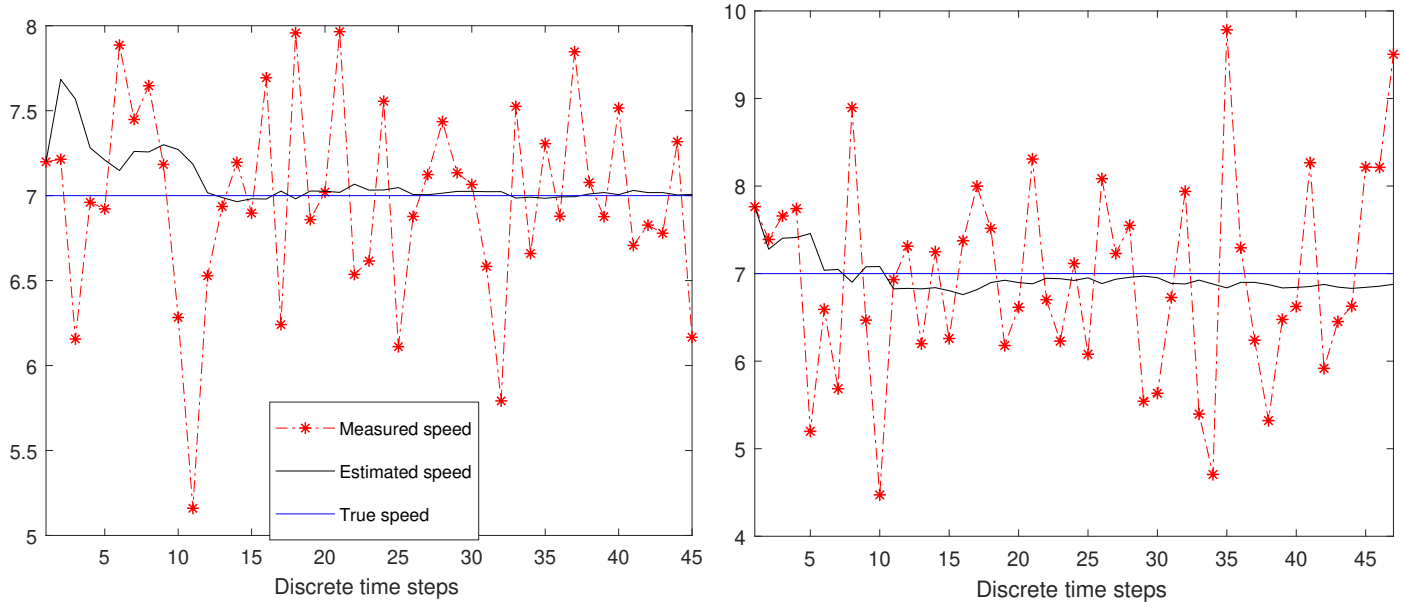

(a) Plots with noise variance $\sigma_x^2, \sigma_y^2, \sigma_k^2$

(b) Plots with noise variance $3\sigma_x^2, 3\sigma_y^2, 3\sigma_k^2$

Figure 4.6: Plots of measured, estimated, true speed

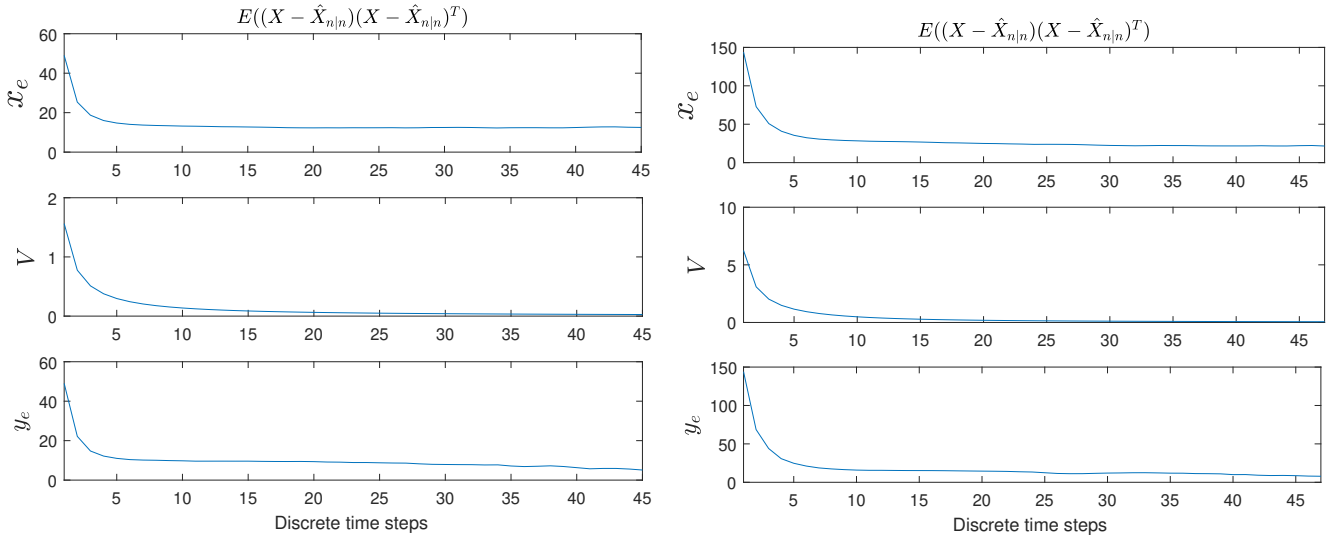

(a) Plots with noise variance $\sigma_x^2, \sigma_y^2, \sigma_k^2$

(b) Plots with noise variance $3\sigma_x^2, 3\sigma_y^2, 3\sigma_k^2$

Figure 4.7: Auto-covariances of states

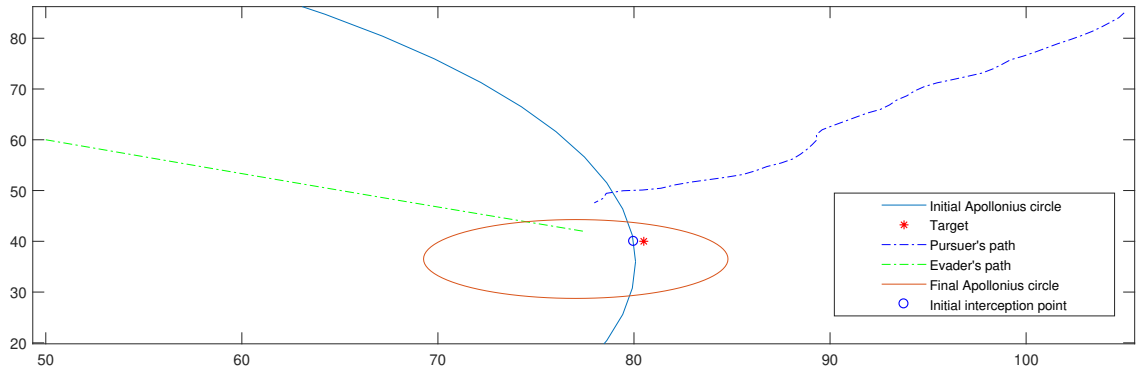

Figure 4.8: Evader wins the game as initial position of pursuer is far from the target.

4.3 Only one feasible evader position results in given interception point as long as game is not won by evader

Let us assume the following distribution for the random variables x_e, y_e, k.

$$f(x) = \begin{cases} \frac{K_x}{2\pi\sigma_x^2} \exp[\frac{-(x-\mu_x)}{\sqrt{2\sigma_x^2}}] & |x| \leqslant 3\sigma_x \\ 0 & |x| \geqslant 3\sigma_x \end{cases} \tag{4.21}$$

where $x \in \{x_e, y_e, k\}$ and K_x is the scaling factor such that $\int_{-\infty}^{+\infty} f(x)dx = 1$. μ_x is the true value of the random variable x i.e., we assume Gaussian noise introduced by the sensor has zero mean.

Let $I_f(\mu_{x_e}, \mu_{y_e}, \mu_k) = (x_I, y_I)$. For the speed ratio μ_k and interception point (x_I, y_I), one of the elements of solution set S is (μ_{x_e}, μ_{y_e}). Let the other solution be (x_e^*, y_e^*). $(x_e^*, y_e^*) \in S_1 \cup S_2$. As long as evader hasn't won the game, any solution belonging to the set S_2 is infeasible because the interception point of element belonging to S_2 is not $I_f(\mu_{x_e}, \mu_{y_e}, \mu_k)$ but $I_f^*(\mu_{x_e}, \mu_{y_e}, \mu_k)$. So we assume $(x_e^*, y_e^*) \in S_1$

If μ_{x_e}, μ_{y_e} and (x_e^*, y_e^*) are probable, then

$$\sqrt{(\mu_{x_e} - x_e^*)^2 + \mu_{y_e} - y_e^*)^2} \leq 3\sqrt{(\sigma_{x_e}^2 + \sigma_{y_e}^2)} \tag{4.22}$$

According to *Result II*, depending on value of μ_k, (4.22) implies one of the following inequalities.

$$\sqrt{(\mu_{x_e} - x_p)^2 + \mu_{y_e} - y_p)^2} < 3\sqrt{(\sigma_{x_e}^2 + \sigma_{y_e}^2)} \tag{4.23}$$

$$\sqrt{(\mu_{x_e} - x_I)^2 + (\mu_{y_e} - y_I)^2} < 3\sqrt{(\sigma_{x_e}^2 + (\sigma_{y_e}^2)} \tag{4.24}$$

Inequality (4.23) is implied when $\mu_k \in [k(\theta_{th}), k(\theta_{max})]$. Inequality (4.24) is implied when $\mu_k \in [k(\theta_{min}), k(\theta_{th})]$.

This means by the time two probable evader locations result in same interception point, the pursuer is close to evader (in which case the game is considered won by pursuer) or evader is close to interception point. If true location of evader is (x_e^*, y_e^*), then evader is going to pursue target. But as long as there is non-zero probability that evader belongs to S_f, pursuer can try to intercept evader at the interception point.

Hence for the rest of the analysis, we assume that only one probable evader location results in the given interception point for a given speed ratio. It is important to note that this assumption only fails when target belongs to dominance region of evader.

Appendix C proves that the feasible and probable evader location is the one that is farthest from the target. So let us define the function $F_E : \mathbb{R}^3 \to \mathbb{R}^2$ as

$$F_E(x_I, y_I, k) = \begin{pmatrix} \mathbb{E}_x(x_I, y_I, k) \\ \mathbb{E}_y(x_I, y_I, k) \end{pmatrix} = (x_e, y_e)$$

where (x_e, y_e) is the feasible and probable evader location resulting in (x_I, y_I), given k. The function F_E[2] is the solution of (2.7), (2.9) that is farthest from the target.

[2] As the expressions of this function are highly complex and give no insight into the problem, they are omitted. These expressions can be derived by solving (2.7) and (2.9) and taking the solution that is farthest from target (ref Appendix C)

4.4 Kalman filter with interception point coordinates and speed ratio, k as states

$$x_{I_n} = f_x(x_e, y_e, x_p, y_p) = \frac{x_{e_n} - x_{p_n}k_n^2}{1-k_n^2} \pm \sqrt{\frac{\frac{k_n^2}{(1-k_n^2)^2}((x_{e_n}-x_{p_n})^2 + (y_{e_n}-y_{p_n})^2)}{1+M^2}},, \tag{4.25}$$

$$y_{I_n} = f_y(x_e, y_e, x_p, y_p) = y_T + M(x_{I_n} - x_T) \tag{4.26}$$

where

$$M = \frac{y_T(1-k_n^2) - (y_{e_n} - y_{p_n}k_n^2)}{x_T(1-k_n^2) - (x_{e_n} - x_{p_n}k_n^2)} \tag{4.27}$$

4.4.1 Difference equations governing interception point dynamics

In the deterministic problem, if both evader and pursuer employ their respective optimal strategies, then interception point is stationary.

$$\frac{dx_I}{dt} = \frac{\partial f_x}{\partial x_e}\frac{dx_e}{dt} + \frac{\partial f_x}{\partial y_e}\frac{dy_e}{dt} + \frac{\partial f_x}{\partial x_p}\frac{dx_p}{dt} + \frac{\partial f_x}{\partial y_p}\frac{dy_p}{dt} = 0 \tag{4.28}$$

$$\begin{aligned}\Rightarrow x_{I_{n+1}} =& x_{I_n} + \frac{\partial f_x}{\partial x_e}(x_{e_{n+1}} - x_{e_n}) + \frac{\partial f_x}{\partial y_e}(y_{e_{n+1}} - y_{e_n}) \\ &+ \frac{\partial f_x}{\partial x_p}(x_{p_{n+1}} - x_{p_n}) + \frac{\partial f_x}{\partial y_p}(y_{p_{n+1}} - y_{p_n}) = x_{I_n}\end{aligned} \tag{4.29}$$

$$\frac{dy_I}{dt} = \frac{\partial f_y}{\partial x_e}\frac{dx_e}{dt} + \frac{\partial f_y}{\partial y_e}\frac{dy_e}{dt} + \frac{\partial f_y}{\partial x_p}\frac{dx_p}{dt} + \frac{\partial f_y}{\partial y_p}\frac{dy_p}{dt} = 0 \tag{4.30}$$

$$\begin{aligned}\Rightarrow y_{I_{n+1}} =& y_{I_n} + \frac{\partial f_y}{\partial x_e}(x_{e_{n+1}} - x_{e_n}) + \frac{\partial f_y}{\partial y_e}(y_{e_{n+1}} - y_{e_n}) \\ &+ \frac{\partial f_y}{\partial x_p}(x_{p_{n+1}} - x_{p_n}) + \frac{\partial f_y}{\partial y_p}(y_{p_{n+1}} - y_{p_n}) = y_{I_n}\end{aligned} \tag{4.31}$$

The assumption is that evader plays optimally at every instant, but pursuer plays sub-optimally. As a result, interception point will no longer be stationary.

Let pursuer's coordinates at $t = n+1$ be (a_n, b_n). Substituting (a_n, b_n) in equa-

tions (4.29) and (4.31) leads to

$$\begin{aligned} x_{I_{n+1}} =& x_{I_n} + \frac{\partial f_x}{\partial x_e}(x_{e_{n+1}} - x_{e_n}) + \frac{\partial f_x}{\partial y_e}(y_{e_{n+1}} - y_{e_n}) \\ &+ \frac{\partial f_x}{\partial x_p}(a_n - x_{p_n}) + \frac{\partial f_x}{\partial y_p}(b_n - y_{p_n}) \neq x_{I_n} \end{aligned} \tag{4.32}$$

$$\begin{aligned} y_{I_{n+1}} =& y_{I_n} + \frac{\partial f_y}{\partial x_e}(x_{e_{n+1}} - x_{e_n}) + \frac{\partial f_y}{\partial y_e}(y_{e_{n+1}} - y_{e_n}) \\ &+ \frac{\partial f_y}{\partial x_p}(a_n - x_{p_n}) + \frac{\partial f_y}{\partial y_p}(b_n - y_{p_n}) \neq y_{I_n} \end{aligned} \tag{4.33}$$

(4.32)-(4.29) $\Rightarrow$

$$x_{I_{n+1}} = x_{I_n} + \frac{\partial f_x}{\partial x_p}(a_n - x_{p_{n+1}}) + \frac{\partial f_x}{\partial y_p}(b_n - y_{p_{n+1}}) \tag{4.34}$$

(4.33)-(4.31) $\Rightarrow$

$$y_{I_{n+1}} = y_{I_n} + \frac{\partial f_y}{\partial x_p}(a_n - x_{p_{n+1}}) + \frac{\partial f_y}{\partial y_p}(b_n - y_{p_{n+1}}) \tag{4.35}$$

where

$$x_{p_{n+1}} = x_{p_n} + (V_p \Delta T)\cos\left(\tan^{-1}\left(\frac{y_{p_n} - y_{I_n}}{x_{p_n} - x_{I_n}}\right)\right) \tag{4.36}$$

$$y_{p_{n+1}} = y_{p_n} + (V_p \Delta T)\sin\left(\tan^{-1}\left(\frac{y_{p_n} - y_{I_n}}{x_{p_n} - x_{I_n}}\right)\right) \tag{4.37}$$

x_{e_n}, y_{e_n} in $\frac{\partial f_x}{\partial x_p}, \frac{\partial f_x}{\partial y_p}, \frac{\partial f_y}{\partial x_p}, \frac{\partial f_y}{\partial y_p}$ are replaced by the expressions $\mathbb{E}_x, \mathbb{E}_y$.

$$\begin{pmatrix} x_{e_n} \\ y_{e_n} \end{pmatrix} = F_E(x_{I_n}, y_{I_n}, k_n) \tag{4.38}$$

Note that if other evader location,$(x^*_{e_n}, y^*_{e_n})$ (i.e., solution belonging to set S_1 for speed ratio k_n and interception point (x_{I_n}, y_{I_n})) is probable and is the actual evader location, then evader has already won the game. So the substitution of (4.38) in (4.34), (4.35) is valid as long as target doesn't fall in the evader's dominance region.

Given the position of pursuer at t[3] $= n+1$, (4.34) and (4.35) predict interception

[3]t refers to time instant

point at $t = n+1$ instant. Note that (a_n, b_n) is where the pursuer will be at $t = n+1$. At $t = n+1$, (a_n, b_n) is used by evader to calculate $(x_{I_{n+1}}, y_{I_{n+1}})$.

Now that we have the difference equations governing interception point dynamics, we can use this model to design a Kalman observer for the system. Let the states of the model be x_I, y_I and k. Define the function G, H, V as follows.

$$G(x_I, y_I, a_n, b_n, x_{p_n}, y_{p_n}, k_n) := x_{I_{n+1}}$$
$$= x_{I_n} + \frac{\partial f_x}{\partial x_p}(a_n - x_{p_{n+1}}) + \frac{\partial f_x}{\partial y_p}(b_n - y_{p_{n+1}}))$$

$$H(x_I, y_I, a_n, b_n, x_{p_n}, y_{p_n}, k_n) := y_{I_{n+1}}$$
$$= y_{I_n} + \frac{\partial f_y}{\partial x_p}(a_n - x_{p_{n+1}}) + \frac{\partial f_y}{\partial y_p}(b_n - y_{p_{n+1}})$$

$$V(x_I, y_I, a_n, b_n, x_{p_n}, y_{p_n}, k_n) := k_{n+1} = k_n$$

as speeds of evader and pursuer are assumed to be constant.

$x_{p_{n+1}}$ and $y_{p_{n+1}}$ are according to equations (4.36) and (4.37) respectively.

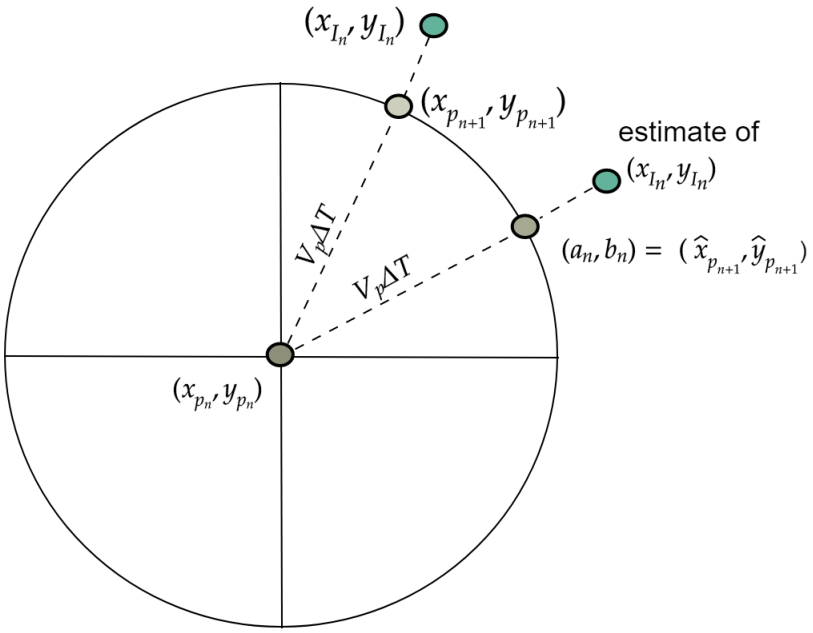

Figure 4.9: Δx_p and Δy_p

$$\begin{pmatrix} x_{I_{n+1}} \\ y_{I_{n+1}} \\ k_{n+1} \end{pmatrix} = \begin{pmatrix} G(x_I, y_I, a_n, b_n, x_{e_n}, y_{e_n}, x_{p_n}, y_{p_n}, k) \\ H(x_I, y_I, a_n, b_n, x_{e_n}, y_{e_n}, x_{p_n}, y_{p_n}, k) \\ V(x_I, y_I, a_n, b_n, x_{e_n}, y_{e_n}, x_{p_n}, y_{p_n}, k) \end{pmatrix} + \begin{pmatrix} \eta \\ \alpha \\ \beta \end{pmatrix}$$

where η, α, β are assumed to be white noise in corresponding states with process error covariance matrix Q, to account for discretization errors.

x_{I_n}, y_{I_n}, k_n are the states and $a_n, b_n, x_{p_n}, y_{p_n}$ are the inputs to the system. x_{e_n}, y_{e_n} are functions of states and inputs.

The dynamics of interception point depends on the pursuer actions which in turn depend on how good the estimates of the interception point are. So the model and observer are intertwined.

4.4.2 Kalman observer model

The model used by the Kalman observer in the estimation process is

$$\hat{x}_{I_{n+1|n}} = \hat{x}_{I_{n|n}} + \frac{\partial \hat{f}_x}{\partial x_p}(a_n - \hat{x}_{p_{n+1}}) + \frac{\partial \hat{f}_x}{\partial y_p}(b_n - \hat{y}_{p_{n+1}})) \tag{4.39}$$

$$\hat{y}_{I_{n+1|n}} = \hat{y}_{I_{n|n}} + \frac{\partial \hat{f}_y}{\partial x_p}(a_n - \hat{x}_{p_{n+1}}) + \frac{\partial \hat{f}_y}{\partial y_p}(b_n - \hat{y}_{p_{n+1}}) \tag{4.40}$$

where

$$\hat{x}_{p_{n+1}} = x_{p_n} + (V_p \Delta T) \cos\left(\tan^{-1}\left(\frac{y_{p_n} - \hat{y}_{I_{n|n}}}{x_{p_n} - \hat{x}_{I_{n|n}}}\right)\right) \tag{4.41}$$

$$\hat{y}_{p_{n+1}} = y_{p_n} + (V_p \Delta T) \sin\left(\tan^{-1}\left(\frac{y_{p_n} - \hat{y}_{I_{n|n}}}{x_{p_n} - \hat{x}_{I_{n|n}}}\right)\right) \tag{4.42}$$

In the Kalman observer, because the states $\hat{x}_{I_n}, \hat{y}_{I_n}$ are the estimates of interception point, $\hat{x}_{I_n}, \hat{y}_{I_n}$ is pursuer by pursuer. Pursuer reaches the estimate of $(x_{p_{n+1}}, y_{p_{n+1}})$, $(\hat{x}_{p_{n+1}}, \hat{y}_{p_{n+1}})$ at $t = n+1$ and so (a_n, b_n) by definition is equal to $(\hat{x}_{p_{n+1}}, \hat{y}_{p_{n+1}})$.

Substituting $(a_n, b_n) = (\hat{x}_{p_{n+1}}, \hat{y}_{p_{n+1}})$ in (4.39), (4.40), we get

$$\begin{aligned} \hat{x}_{I_{n+1|n}} &= \hat{x}_{I_{n|n}} \\ \hat{y}_{I_{n+1|n}} &= \hat{y}_{I_{n|n}} \end{aligned} \tag{4.43}$$

As the input (a_n, b_n) is a function of states and other inputs in Kalman observer model, (a_n, b_n) linearises the system. But in the actual system this is not the case. The sub-optimal play of the pursuer is the cause of dynamics in interception point. But according to Kalman filter, at each step, pursuer is playing optimally and so prediction step in Kalman filter is rendered redundant.

Hence the model used by Kalman filter is $\hat{X}_{n+1|n} = A\hat{X}_{n|n}$, where A is identity matrix of order 3.

Prediction error covariance matrix,

$$P_{n+1|n} = AP_{n|n}A^T + Q$$

Output:

Pursuer gets readings of x_{e_n}, y_{e_n}, k_n. We can find the output matrix C_n by linearizing $\mathbb{E}_x$ and $\mathbb{E}_y$ at $(\hat{x}_{I_{n|n}}, \hat{y}_{I_{n|n}}, \hat{k}_{n|n}, x_{p_n}, y_{p_n})$.

$$Z = \begin{pmatrix} x_{e_m} \\ y_{e_m} \\ k_m \end{pmatrix}_n = \begin{pmatrix} \mathbb{E}_x(x_{I_n}, y_{I_n}, k_n) \\ \mathbb{E}_y(x_{I_n}, y_{I_n}, k_n) \\ k_n \end{pmatrix} + \begin{pmatrix} \eta_m \\ \alpha_m \\ \beta_m \end{pmatrix} \tag{4.44}$$

$$C_n = \begin{pmatrix} \frac{\partial \mathbb{E}_x}{\partial x_e} & \frac{\partial \mathbb{E}_x}{\partial y_e} & \frac{\partial \mathbb{E}_x}{\partial k_e} \\ \frac{\partial \mathbb{E}_y}{\partial x_e} & \frac{\partial \mathbb{E}_y}{\partial y_e} & \frac{\partial \mathbb{E}_y}{\partial k_e} \\ 0 & 0 & 1 \end{pmatrix}_{(\hat{x}_{I_{n|n-1}}, \hat{y}_{I_{n|n-1}}, \hat{k}_{e_{n|n-1}}, x_{p_n}, y_{p_n})} \tag{4.45}$$

where $\begin{pmatrix} x_{e_m} \\ y_{e_m} \\ k_m \end{pmatrix}_n$ is vector of evader's position and speed measurements at $t = n$. $\eta_m, \alpha_m, \beta_m$ are assumed to be i.i.d noise in corresponding states with measurement error covariance matrix R.

$$R = \begin{pmatrix} \sigma_{x_e}^2 & 0 & 0 \\ 0 & \sigma_{y_e}^2 & 0 \\ 0 & 0 & \sigma_k^2 \end{pmatrix}$$

where $\sigma_{x_e}, \sigma_{y_e}, \sigma_k$ are standard deviations of x_e, y_e, k respectively.

States Initialization

$$\begin{pmatrix} \hat{x}_{I_{0|0}} \\ \hat{y}_{I_{0|0}} \end{pmatrix} = I_f(x_{e_0}, y_{e_0}, k_0)$$

k_0 is the initial measurement of the state k. $\hat{k}_{0|0} = k_0$

P matrix is initialized such that it is approximates the auto and cross co-variance values of initial interception point coordinates and speed of evader. Choice of initial P matrix is not critical as it only affects the initial estimates of EKF unless it is out of acceptable limits [7].

4.4.3 Simulation results

Simulations of game[4] have been performed and the results are thoroughly analyzed.

Note that pursuer is considered to have won the game if by the time pursuer is within vicinity radius D of the evader, target is in pursuer's dominance region.

Pursuer and evader employ the decision making algorithms (4.1) and (4.2) respectively except that in this approach, pursuer estimates the interception point location and heads toward it. The plots of paths followed by evader and pursuer are

[4] the same example considered in chapter 4 to analyze the Kalman filter designed for estimating evader's position and speed

shown in 4.9. Pursuer is able to intercept the evader at a point very close to the initial interception point.

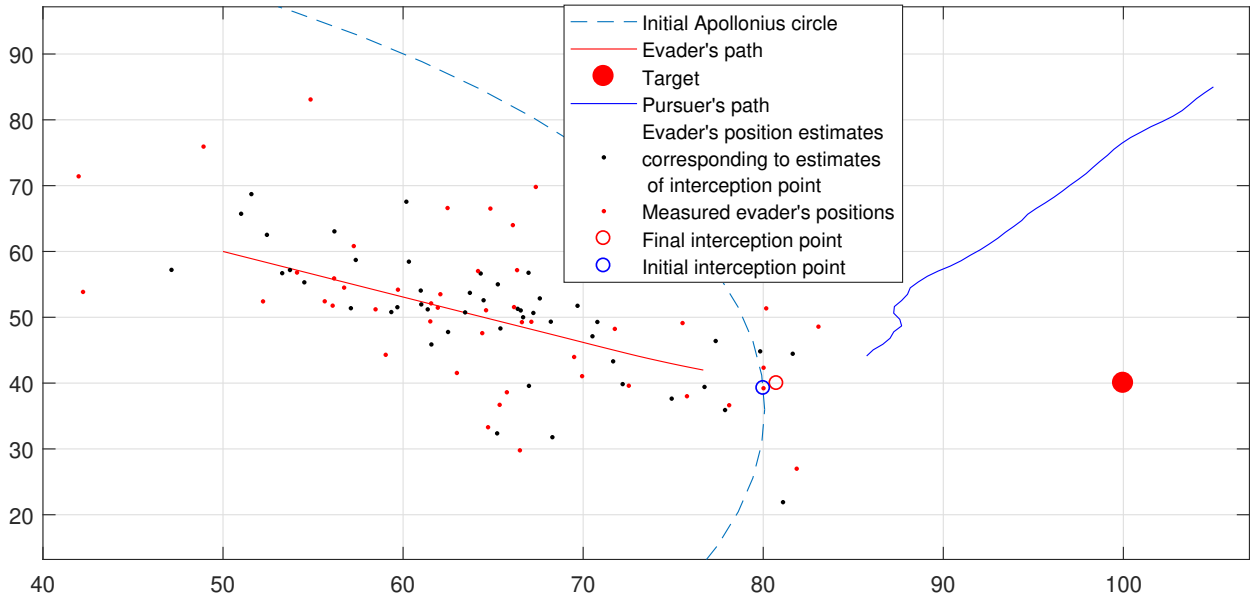

Figure 4.10: Pursuer won this game as he reached within a pre-specified distance, D from evader

The auto-covariance plots of the states reveal the complete performance of the Kalman filter for this system. As can be seen from the plots of 4.11, auto-covariance of speed of evader[5] reached a non-zero steady state value approximately after $n = 20$ which means that the Kalman filter couldn't improve further the estimates of k using the measurements (refer plot 4.10). Also the convergence time of the speed of evader estimate to true value is smaller for $KF1$ compared to that of $KF2$. Comparing the performance of the Kalman filter ($KF2$) with the performance of Kalman filter designed in chapter 4 ($KF1$), estimating the evader's position and speed and pursuing the corresponding interception point gives better performance (in terms of convergence to true value) than estimating directly the instantaneous interception point. The estimates of states x_I, y_I are poorer (as game reached the end) compared to the estimates of x_e, y_e by $KF1$. So if the vicinity radius D is small and target is closer to the initial interception point, the probability of pursuer losing the game is higher when pursuer uses $KF2$ than when he uses $KF2$.

[5]State k and speed of evader differ by a constant multiple. Plots related to evader's speed are presented here for ease of understanding

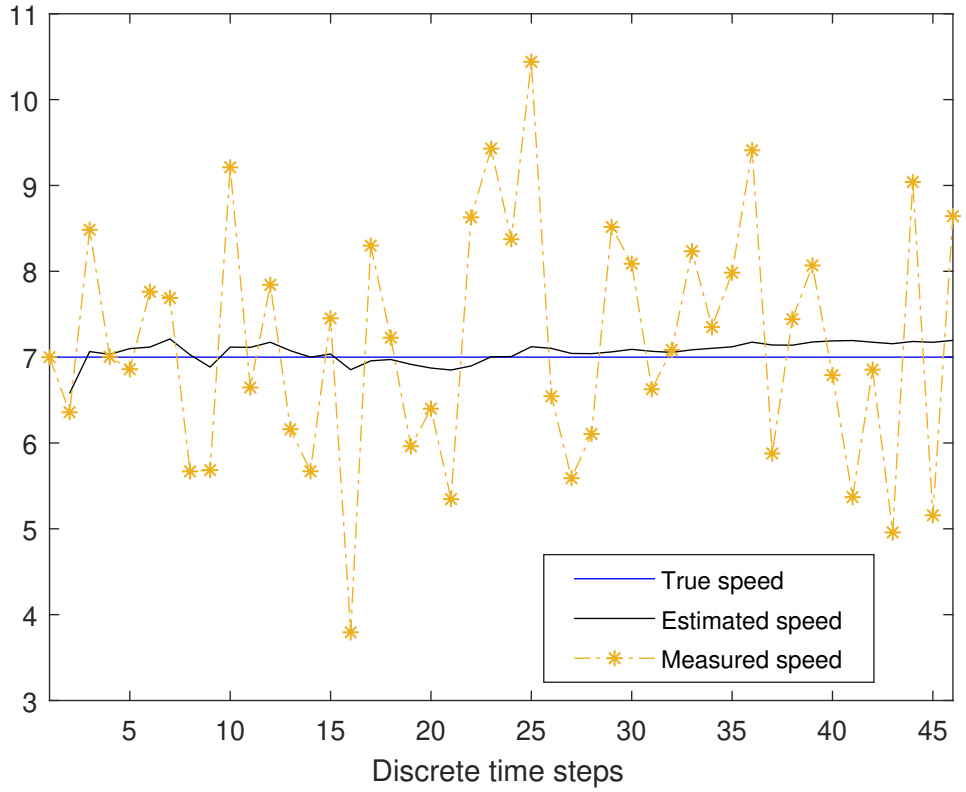

Figure 4.11: Plots of estimated, measured and true values of speed ratio Estimated speed ratio follows the variations in measurements

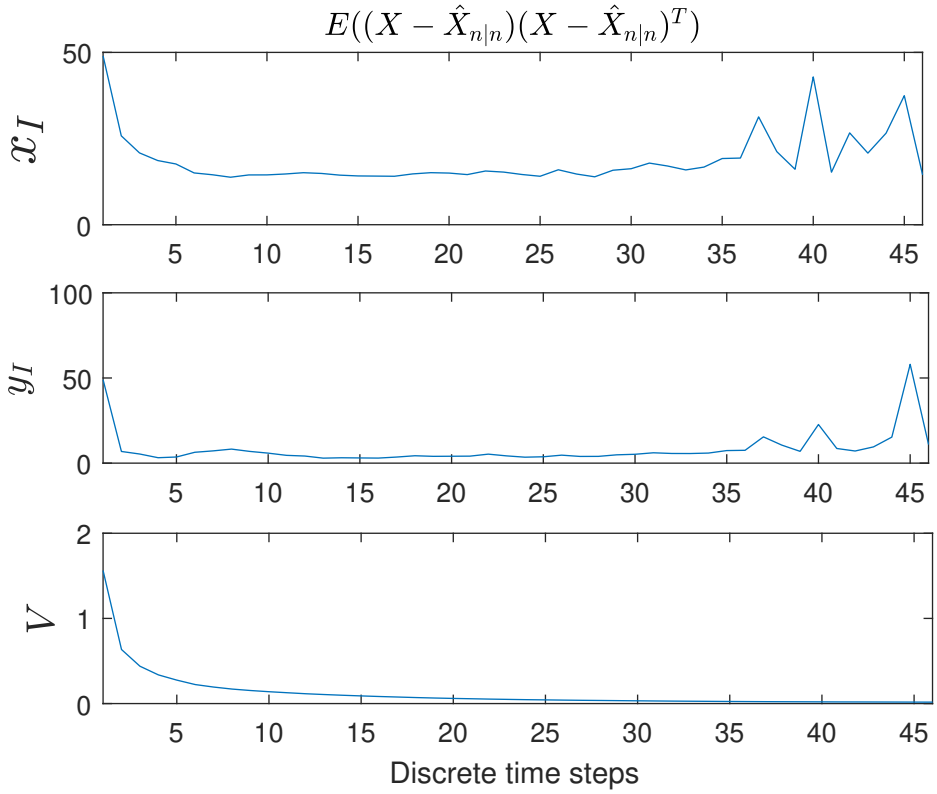

Figure 4.12: Auto-covariance plots of states

CHAPTER 5

Miscellaneous approaches

5.1 Introduction

In chapter 4 we presented Kalman filtering approach that filters the noise present in the measurements. Usually, instead of single sensor, multiple sensors are used to measure the position and speed of evader. At every instant pursuer gets the measurements from the sensors and so the average and standard deviation of these readings can be known. According to central limit theorem, if each of the readings from sensors is assumed to be corrupted by Gaussian noise, then the average and standard deviation of all the readings from sensors give the true mean and standard deviation of the Gaussian distributed measurand. In this chapter, we examine two approaches, namely mean pursuit and most probable point pursuit. These strategies are not implemented on the developed testbed because of their computationally-intensive algorithms. So the study of these two strategies is based only on the simulation results.

We assume the following density functions for the random variables x_e, y_e, k for rest of the analysis.

$$f(x) = \begin{cases} \frac{K_x}{2\pi\sigma_x^2} \exp[\frac{-(x-\mu_x)}{\sqrt{2\sigma_x^2}}] & |x| \leqslant n\sigma_x \\ 0 & |x| \geqslant n\sigma_x \end{cases} \tag{5.1}$$

where $x \in \{x_e, y_e, k\}$ and K_x is the scaling factor such that $\int_{-\infty}^{+\infty} f(x)dx = 1$. n-σ_x is the confidence level assumed for random variable x. μ_x is the mean value of the random variable x. Note that μ_x is not the true value of the random variable. This forms a cuboid region for the set of all probable points of evader position and speed. Let this region be $\mathscr{R}$.

5.2 Mean interception point pursuit

Let the coordinates of evader, pursuer, target respectively be (x_e, y_e), (x_p, y_p), (x_T, y_T). The corresponding interception point be at (x_I, y_I). Let us denote the expressions for the coordinates of interception point, (5.2), (5.3) as $I_x(x_e, y_e, k), I_y(x_e, y_e, k)$.

$$x_I = I_x(x_e, y_e, k) = \frac{x_e - x_p k^2}{1 - k^2} \pm \sqrt{\frac{((x_e - x_p)^2 + (y_e - y_p)^2)\frac{k^2}{(1-k^2)^2}}{1 + (\frac{y_T(1-k^2) - y_e + y_p k^2}{x_T(1-k^2) - x_e + x_p k^2})^2}}, \tag{5.2}$$

$$y_I = I_y(x_e, y_e, k) = \frac{y_e - y_p k^2}{1 - k_e^2} \pm \sqrt{\frac{((x_e - x_p)^2 + (y_e - y_p)^2)\frac{k^2}{(1-k^2)^2}}{1 + (\frac{x_T(1-k^2) - x_e + x_p k^2}{y_T(1-k^2) - y_e + y_p k^2})^2}} \tag{5.3}$$

Let the functions I_x, I_y map the region $\mathscr{R}$ to the region $\mathscr{I}$. As we know the average values and standard deviations of x_e, y_e, k, we can find the mean of the interception point from the formulae.

$$\begin{aligned}
\mu_x &= \int_{-\infty}^{+\infty}\int_{-\infty}^{+\infty}\int_{-\infty}^{+\infty} I_x(x_e, y_e, k) F(x_e, y_e, k) dx_e\, dy_e\, dk \\
\mu_y &= \int_{-\infty}^{+\infty}\int_{-\infty}^{+\infty}\int_{-\infty}^{+\infty} I_y(x_e, y_e, k) F(x_e, y_e, k) dx_e\, dy_e\, dk \\
\mu_\alpha &= \int_{-\infty}^{+\infty}\int_{-\infty}^{+\infty}\int_{-\infty}^{+\infty} tan^{-1}\left(\frac{I_y(x_e, y_e, k) - y_p}{I_x(x_e, y_e, k) - x_p}\right) F(x_e, y_e, k) dx_e\, dy_e\, dk
\end{aligned} \tag{5.4}$$

where μ_x, μ_y are mean values of x and y coordinates of interception point respectively. μ_α is the mean heading angle. $F(x_e, y_e, k)$ is the joint distribution function of the independent random variables x_e, y_e, k.

$$F(x_e, y_e, k) = f(x_e) f(y_e) f(k)$$

Let the functions I_x, I_y map the region $\mathscr{R}$ to the region $\mathscr{I}$. As the functions I_x, I_y are highly non-linear, it is not possible to characterize the set $\mathscr{I}$ and so is difficult to comment on its convexity. The mean interception point (μ_x, μ_y) can lie outside the set $\mathscr{I}$. This means for the interception point pursued by pursuer, there need not exist an inverse point lying in the region $\mathscr{R}$. But pursuing mean point can lead him

towards the region $\mathscr{I}$.

Note that as pursuer is finding (μ_x, μ_y) at every instant and heading towards it, his decision at every instant is affected by evader locations whose regions of dominance contain the target (if target is inside the region $\mathscr{I}$, it means that there are evader position-speed combinations with non-zero probability whose corresponding dominance regions include target).

Define D as the minimum distance between pursuer and evader required for the pursuer to get uncorrupted measurements of evader's position and speed. Pursuer is considered to have won the game if by the time he is within distance D from evader, target is not in evader's dominance region.

5.2.1 Simulation results

Simulations of the game for two different values of D are presented in this section.

- Let $D = D_1$. Pursuer is able to intercept the evader before evader is too close to the target (refer Fig 5.1). The initial interception point and final interception point pursued by evader are very close.

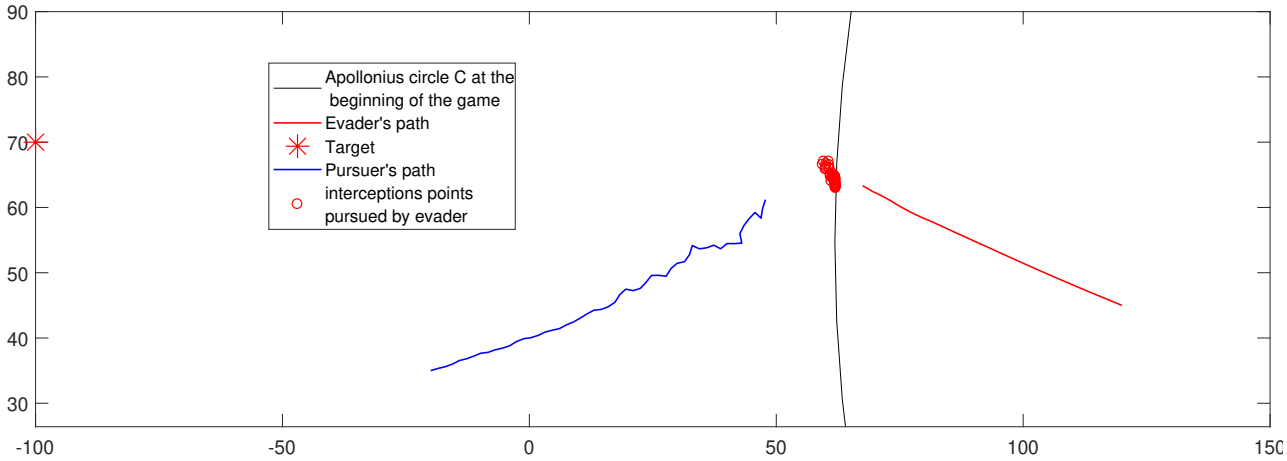

Figure 5.1: Plot showing the suboptimal path of when pursuer heads towards instantaneous mean interception point. $D = D_1$

- Let $D = D_2$[1] $< D_1$. In this case also, pursuer is able to intercept the evader but only after evader reaches much closer point to target than he does when $D = D_1$. This is expected because $D_2 < D_1$. So when pursuer uses mean point pursuit, D has to be very high in order for him to protect the target before target falls in evader's dominance region.

[1] D considered in $KF1$ and $KF2$ is less than D_2

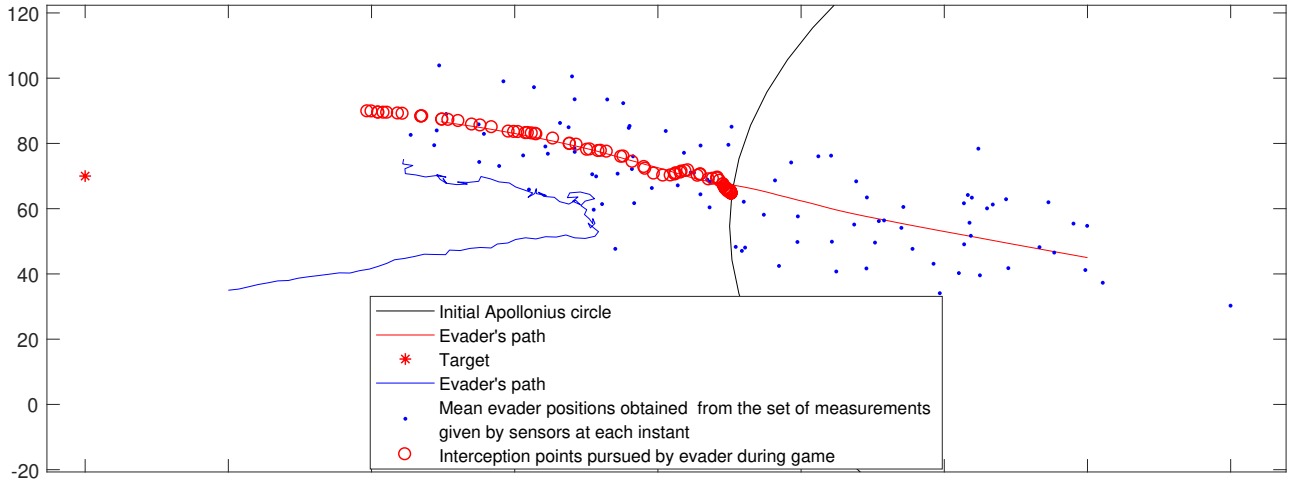

Figure 5.2: Plot showing the suboptimal path of pursuer when pursuer heads towards instantaneous mean interception point. $D = D_2 < D_1$

5.3 Heading along μ_α

Let pursuer heads with heading angle equal to mean heading angle at every instant.

We investigate this strategy to see whether pursuer can intercept evader before target falls in evader's dominance region.

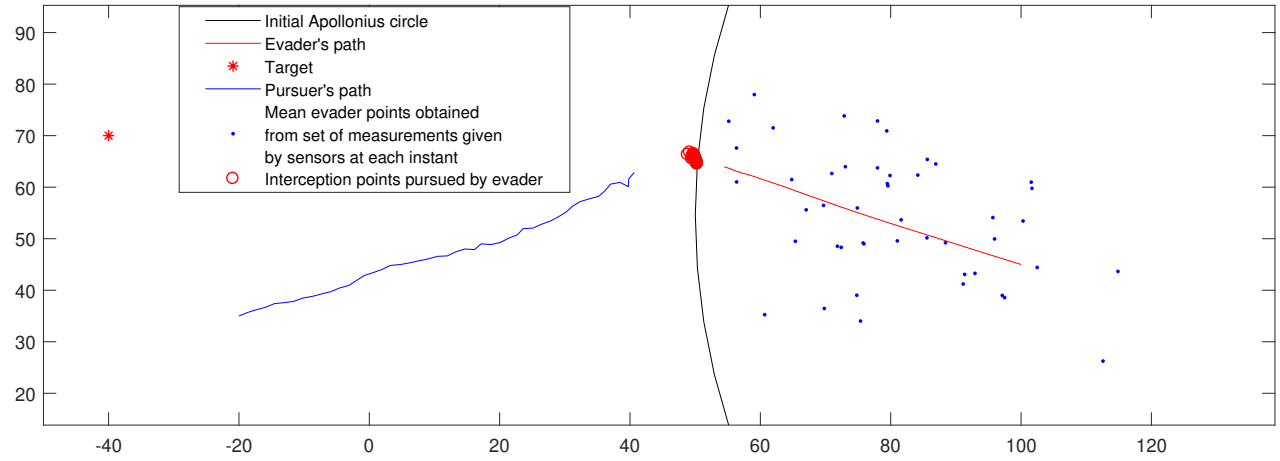

Figure 5.3: Plot showing the suboptimal path of pursuer when pursuer heads with mean heading angle at every instant. $D = D_1$. As D_1 is large enough, pursuer is able to intercept evader.

- When $D = D_2 < D_1$, unlike in mean interception point pursuit case, pursuer is able to intercept evader before evader reaches very close to target. So we conclude heading along mean heading direction is a better strategy compared to mean interception point pursuit.

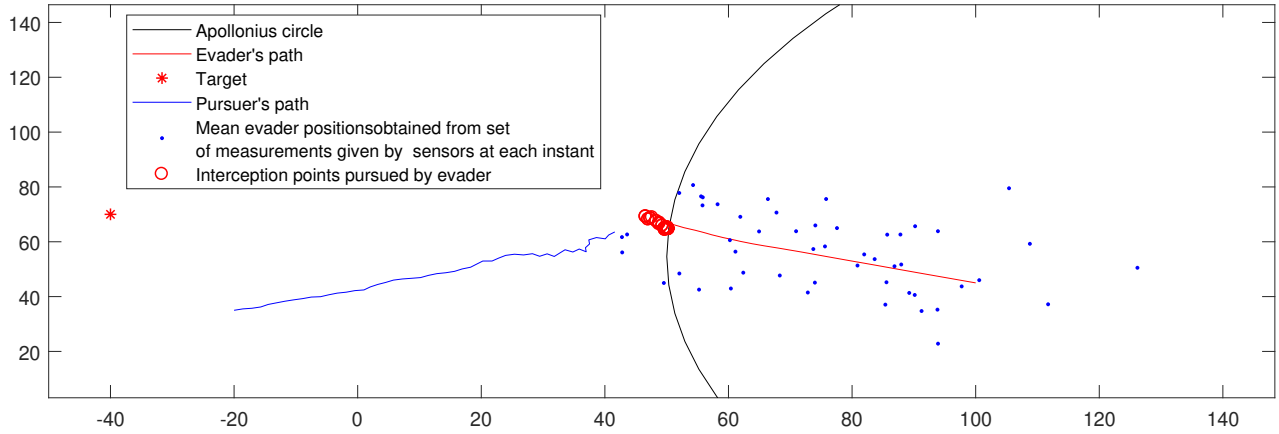

Figure 5.4: Pursuer is able to intercept evader at a point very close to initial interception point. $D = D_2 < D_1$

5.4 Characterization of $\mathbb{S}_f, \mathbb{S}_1, \mathbb{S}_2$,

In chapter 2, we studied the geometry of the game and found the set of all evader locations which result in the same interception point. We defined this set as $\mathbb{S}_f$. In this section, we characterize this set and find the probability density map of (x_I, y_I).

Set $\overline{S}$ is the set of all evader positions and speeds satisfying the equations (2.17), (2.20) (reproduced below for quick reference).

$$C_m : (x_e - x_{cm})^2 + (y_e - y_{cm})^2 = R_m^2 \tag{5.5}$$

$$k^2 = \frac{(x_e - x_I)^2 + (y_e - y_I)^2}{((x_p - x_I)^2 + (y_p - y_I)^2)} \tag{5.6}$$

where

$$x_{cm} = x_I - \frac{HM}{2}, y_{cm} = y_I + \frac{H}{2}$$

$$R_m^2 = (x_I - x_{cm})^2 + (y_I - y_{cm})^2 = \frac{H^2(M^2+1)}{4}$$

$$H = \frac{(x_p - x_I)^2 + (y_p - y_I)^2}{(y_p - Mx_p - c)}$$

$$M = \frac{y_T - y_I}{x_T - x_I}$$

$$c = y_T - x_T;$$

Parametric equations corresponding to (5.5) and (5.6) are

$$x_e(\theta) = x_{cm} + R_m \cos\theta \tag{5.7}$$

$$y_e(\theta) = y_{cm} + R_m \sin\theta \tag{5.8}$$

$$k(\theta) = \frac{\sqrt{(x_I - (x_{cm} + R_m\cos\theta))^2 + (y_I - (y_{cm} + R_m\sin\theta))^2}}{\sqrt{(x_I - x_p)^2 + (y_I - y_p)^2}} \tag{5.9}$$

where

$$\theta = \tan^{-1}\left(\frac{y_e - y_{cm}}{x_e - x_{cm}}\right) \tag{5.10}$$

We defined $\theta_{min}, \theta_{max}$ in section 2.5 as

$$\theta_{max} = \arg\max_{\theta} k(\theta)$$

$$\theta_{min} = \arg\min_{\theta} k(\theta)$$

$$\theta_{th} = \frac{\theta_{min} + \theta_{max}}{2}$$

Assuming $\theta_{min} < \theta_{max}$, from Appendix B, $\theta_{max} - \theta_{min} = 180^0$. This means the line joining $(x_e(\theta_{min}), y_e(\theta_{min}))$ and $(x_e(\theta_{max}), y_e(\theta_{max}))$ is a diameter to the circle C_m. Let the equation of this line be

$$L_\theta : y - m_\theta x - c_\theta = 0$$

Note that $m_d \times M = -1$ i.e., line L (2.7) is perpendicular to L_θ.

The hyperplane L_θ separates the 2-dimensional Cartesian space, $\mathbb{R}^2$ into two half planes.

$$\mathbb{R}^2_1 : y - m_\theta x - c_\theta < 0$$

$$\mathbb{R}^2_2 : y - m_\theta x - c_\theta > 0$$

Let $(x_T, y_T) \in \mathbb{R}^2_i$ where $i = 1\ or\ 2$. Let us define two sets $\mathscr{A}_1, \mathscr{A}_2$ as

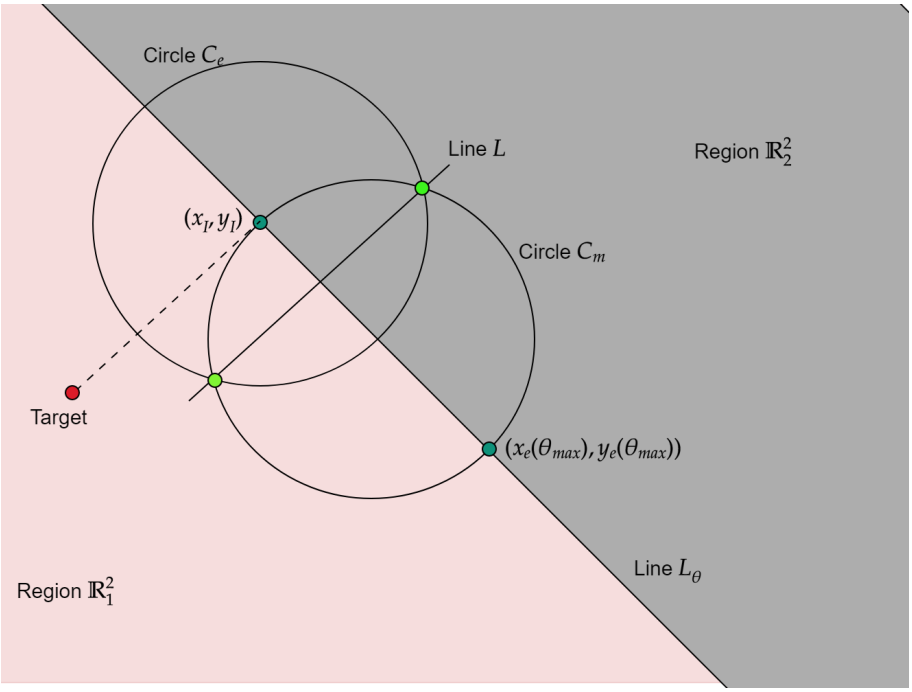

Figure 5.5: C_m, C_e, L_θ, L are such that $L_\theta \perp L$

$$\mathscr{A}_1 = \{(x,y)|(x,y) \in C_m, (x,y) \in \mathbb{R}_i^2\}$$

$$\mathscr{A}_2 = \{(x,y)|(x,y) \in C_m, (x,y) \in \mathbb{R}_j^2, j \neq i\}$$

Suppose $(x_T, y_T) \in \mathbb{R}_1^1$. $\mathscr{A}_1$ is set of all points lying on the circle C_m in the region $\mathbb{R}_1^2$ and $\mathscr{A}_2$ is set of all points lying on the circle C_m in the region $\mathbb{R}_2^2$

Out of the two elements of the set S, the element that is farthest from target belongs to S_f (refer Appendix C). Extending this result to to case where k is also variable, we find that the elements of set $\mathscr{A}_2$ belongs to $\mathbb{S}_f$. Hence, identities (5.11) and (5.12) follow.

$$\mathbb{S}_f \equiv \mathscr{A}_2 \tag{5.11}$$

$$\mathbb{S}_1 \cup \mathbb{S}_2 \equiv \mathscr{A}_1 \tag{5.12}$$

Note that target demarcates the centers of $\mathbb{S}_1, \mathbb{S}_2$ (refer Fig 2.6). So position of target is enough to segregate the set $\mathscr{A}_1$ into $\mathbb{S}_1$ and $\mathbb{S}_2$

5.5 Finding probability density map of (x_I, y_I)

Given (x_I, y_I, θ), corresponding (x_e, y_e, k) can be calculated from the equations (5.7), (5.8), (5.9). (x_I, y_I, θ) corresponding to the given (x_e, y_e, k) can be calculated from the equations (5.2), (5.3), (5.10). This implies we can find the Jacobian of the transformation $T: (x_I, y_I, \theta) \rightarrow (x_e, y_e, k)$ from the formula (5.13).

$$J\left(\frac{x_e, y_e, k}{x_I, y_I, \theta}\right) = \begin{pmatrix} \frac{\partial x_e}{x_I} & \frac{\partial y_e}{x_I} & \frac{\partial k}{x_I} \\ \frac{\partial x_e}{y_I} & \frac{\partial y_e}{y_I} & \frac{\partial k}{y_I} \\ \frac{\partial x_e}{\theta} & \frac{\partial y_e}{\theta} & \frac{\partial k}{\theta} \end{pmatrix} \tag{5.13}$$

The joint probability distribution function of the random variables (x_I, y_I, θ) can be determined from the formula (5.14)

$$F_T(x_I, y_I, \theta) = J\left(\frac{x_e, y_e, k}{x_I, y_I, \theta}\right) F(T^{-1}(x_e, y_e, k)) \tag{5.14}$$

where $T^{-1}: (x_e, y_e, k) \rightarrow (x_I, y_I, \theta)$

The set of all evader positions along with associated speeds which result in given interception point (x_I, y_I) is $\mathbb{S}_f \cup \mathbb{S}_1$. The intersection of the region $\mathscr{R}$ (defined in section 5.1) with $\mathbb{S}_f \cup \mathbb{S}_1$ gives the set of all evader positions along with the associated speeds, $\{(x_e, y_e, k)\}$ with non-zero probabilities which result in interception point (x_I, y_I).

Given (x_I, y_I), we can find $\overline{S}$ and hence we can find the sets $\mathbb{S}_f, \mathbb{S}_1, \mathbb{S}_2$. Also from section 2.4, we know that the function I_f is continuous over $\mathbb{S}_f, \mathbb{S}_1, \mathbb{S}_2$. The elements of the set $\mathbb{S}_f, \mathbb{S}_1$ are functions of θ (We parametrized the set $\overline{S}$ in section 2.4). So bounded curve $\mathscr{R} \cap (\mathbb{S}_f \cup \mathbb{S}_1)$ gives the boundary values of θ. Let these boundary values be $\overline{\theta_1}, \overline{\theta_2}$ with $\overline{\theta_1} \leq \overline{\theta_2}$

Using $F_T(x_I, y_I, \theta)$ from (5.14), we can find the probability density of any *given*

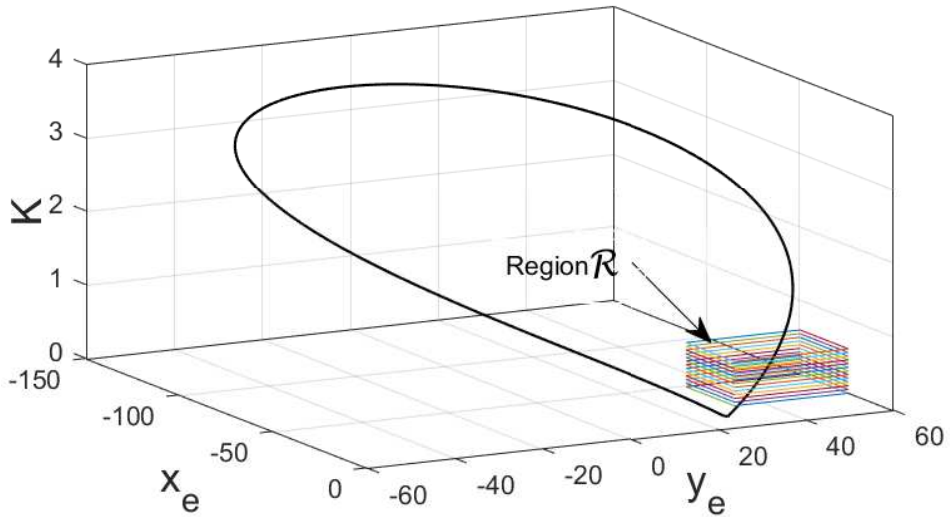

Figure 5.6: Intersection of solution set S with region $\mathscr{R}$

interception point (x_I, y_I) from the marginal density formula (5.15)

$$\overline{F}_I(x_I, y_I) = \int_{\mathscr{R}\cap(\mathbb{S}_f\cup\mathbb{S}_1)} F_T(x_I, y_I, \theta)\ d\theta = \int_{\theta_1}^{\overline{\theta_2}} F_T(x_I, y_I, \theta)\ d\theta \tag{5.15}$$

Unlike in the mean point pursuit approach, we can make pursuer's decisions unaffected by solutions of the set $\mathbb{S}_1$ by integrating over $\mathscr{R}\cap(\mathbb{S}_f)$ instead of integrating over $\mathscr{R}\cap(\mathbb{S}_f\cup\mathbb{S}_1)$. By not integrating over $\mathscr{R}\cap(\mathbb{S}_f\cup\mathbb{S}_1)$, we are considereing feasible and probable solutions of set $\overline{S}$. Let the new bounds on θ be θ_1, θ_2 with $\theta_1 \le \theta_2$.

$$F_I(x_I, y_I) = \int_{\mathscr{R}\cap\mathbb{S}_f} F_T(x_I, y_I, \theta)\ d\theta = \int_{\theta_1}^{\theta_2} F_T(x_I, y_I, \theta)\ d\theta \tag{5.16}$$

Note that we can use (5.16) only if we know θ_1, θ_2. But θ_1, θ_2 depend on the transformation T which in turn depends on (x_I, y_I).

5.6 Most probable point pursuit

Before proceeding, let us define sets $\mathcal{N}_a$, $\mathcal{N}$, I as

$$\mathcal{N}_a = \{a | a \in \{-n\sigma_a + \mu_a, -(n-1)\sigma_a + \mu_a ..... \mu_a ..... (n-1)\sigma_a + \mu_a, n\sigma_a + \mu_a\}\}$$

$$\mathcal{N} = \mathcal{N}_{x_e} \times \mathcal{N}_{y_e} \times \mathcal{N}_k$$

$$I = \{(x_I, y_I) | I_f(x_e, y_e, k) = (x_I, y_I) \forall (x_e, y_e, k) \in \mathcal{N}\} \tag{5.17}$$

where μ_a, σ_a are mean and standard deviation of the random variable a. $\mathcal{N}_a$ is set of all values of a at confidence levels $\pm\sigma_a, \pm 2\sigma_a, \pm 3\sigma_a ..... \pm n\sigma_a$. Note that $\mathcal{N} \subset \mathcal{R}$.

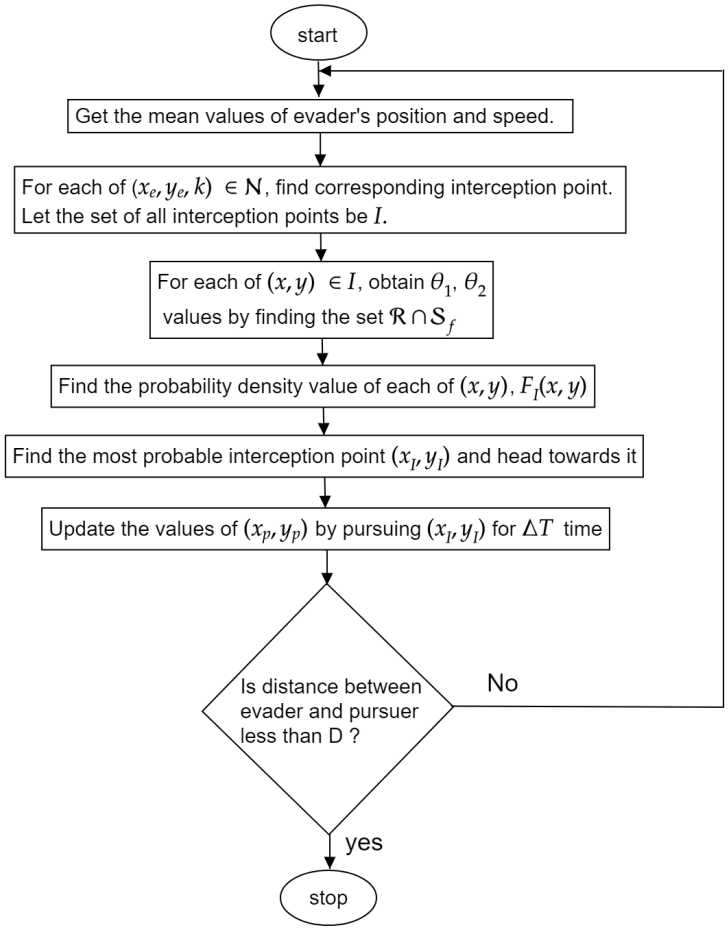

Figure 5.7: Flowchart showing the decision making algorithm of pursuer

The algorithm in this approach can be well explained through the flowchart 5.7. Pursuer pursues the interception point whose probability density value is highest,

$(x_I, y_I)_M$ at every instant of time, where

$$(x_I, y_I)_M = \arg\max_I F_I(x_I, y_I)$$

until he reaches within D distance from evader.

Note that we are finding interception point with highest F_I instead of $\overline{F}_I$. This way we can make pursuer's decision not affected by probable position-speed combinations of evader whose dominance regions contain target.

5.6.1 Simulation results

Three examples are presented to draw conclusions from the performance of this strategy and to compare with the other strategies presented so far.

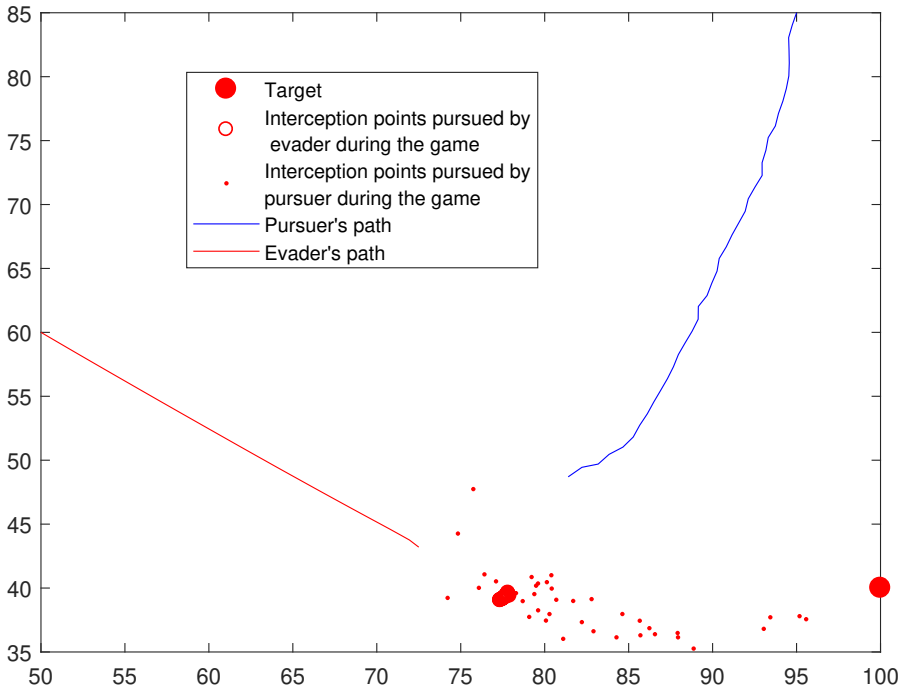

Figure 5.8: Game-I

In all three games, pursuer is able to intercept evader before he reaches close to target even though pursuer is initially away from the target (refer game-I). From the results, we conclude that both heading along μ_α and pursuit of interception point with highest density strategies render almost same performance. The former strategy is computationally more efficient and so is practically employable. Even though

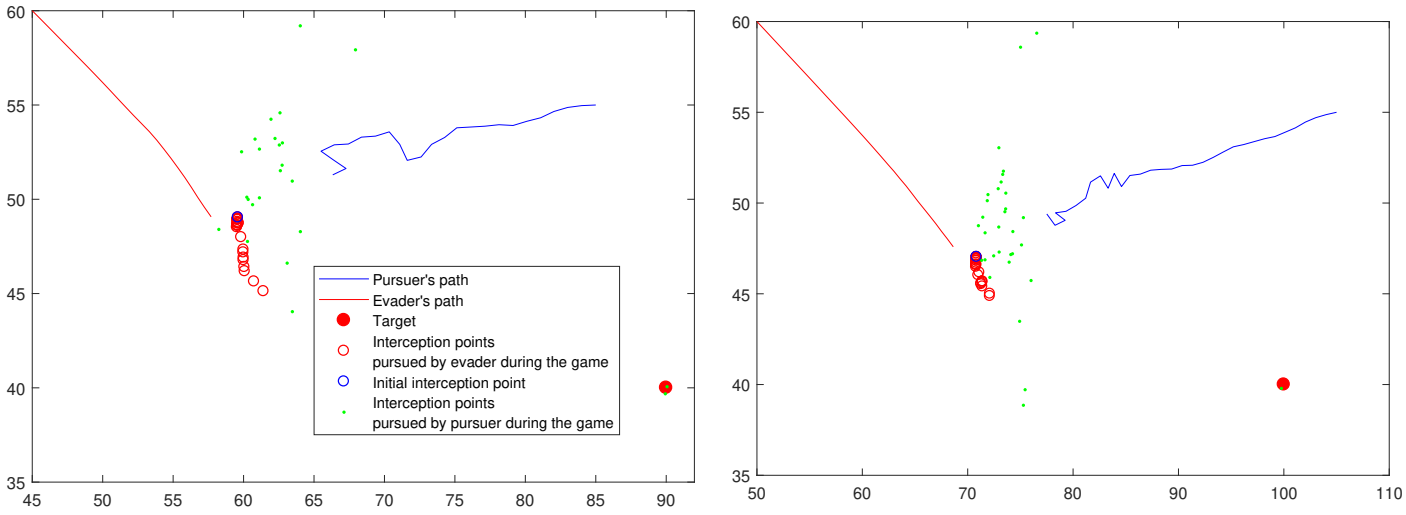

(a) Game-II (b) Game-III

Figure 5.9: plots of pursuer's path and evader's path

Bayesian Nash equilibrium strategy could be the best strategy for pursuer to employ, it demands huge computational resources and so if means and variances of evader's position and speed are known, best strategy (considering the computational effort) for pursuer is to head along μ_α.

CHAPTER 6

Experimental results

6.1 A test bed for implementing control laws in a two player difference game

We build an algorithm testing platform using LEGO Mindstorms kits and validate the performance of Kalman Observers designed in chapter 4. The platform consists of two LEGO robots and a ceiling mounted camera with a bird's-eye view. Each LEGO robot has a differential drive system with PID controllers for each of the two motors which precisely control the motion of the robot. Matlab supports NatNet SDK which is a set of client/server library used to access the data from motion tracking system. Tracking data from cameras is streamed in an optical motion capture software provided by OptiTrack called Motive. Calibration of play field is done in this software. The commands generated by the control law under validation are used to calculate the desired position and yaw angle of robot. The desired position and yaw of robot are used to generate control commands for robots to correct the position and yaw of the robot which are tracked in Motive software.

6.1.1 Tracking and controlling the robots

Retro-reflective markers are mounted on robot and a rigid body is created in Motive. Motive finds the centroid of the rigid body and streams the position and quaternion angles to be used in Matlab through NatNet SDK library. Asymmetry is the key to avoiding the congruency for tracking multiple marker sets. For example, a perfect square marker arrangement will have ambiguous orientation and frequent mislabels

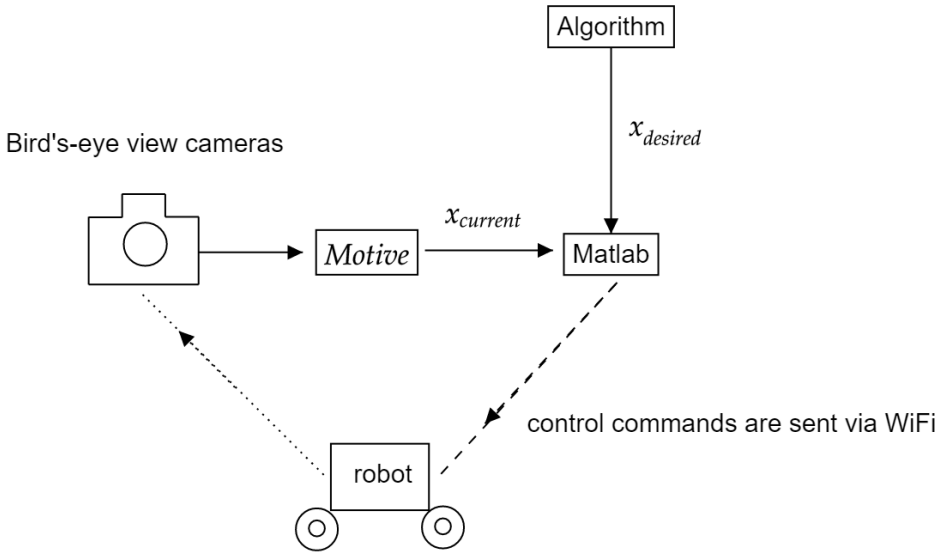

Figure 6.1: Block diagram showing how the position and yaw angle of robot are controlled

may occur throughout the capture. In order to track all the yaw angles without ambiguity and differentiate between two rigid bodies, markers are mounted asymmetrically.

Figure 6.1 depicts how control commands are communicated to robot to achieve the desired position and orientation. Placement of markers is shown in Figure 6.2.

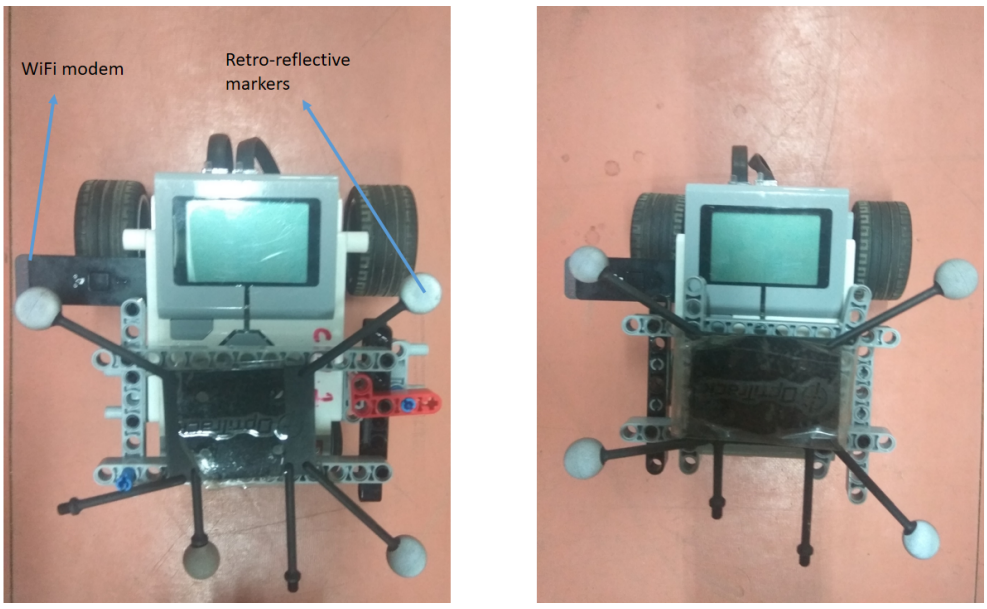

Figure 6.2: Markers are placed asymmetrically on each of the two robots used for experiments

6.2 Practical considerations

So far, in devising strategies for the pursuer to win the game in-spite of the unavailability of perfect information of evader's position and speed, we have assumed both players to be zero-dimensional robots with infinite turn rate. Neither of these assumptions hold true in real time and so the optimal strategies are affected by size and turn rate of players. The time taken for the robot to align in the instantaneous optimal heading angle direction affects the overall performance of the player. Also while turning the translation speed of the robot need not be zero. After the robot aligns in the optimal heading angle direction, the position of the robot changes and heading angle of the robot need not be optimal with respect to its new position. These two non-idealities are modelled as Gaussian noise in the system and can be accounted for through the process noise covariance matrix Q.

Data acquisition:

As the in-house ceiling mounted cameras measure position accurate upto millimetre, Gaussian noise is added to the acquired measurement data.

6.3 Experimental results

Evader may lose an otherwise winning game even if pursuer is playing sub-optimally because of practical limitations causing evader to take sub-optimal path. Same is the case with pursuer. Figure 6.3 shows that the distance between target and final interception point is higher than in simulation. Both the robots deviate from their respective simulation paths. If limitations on pursuer's motion do not allow free maneuver of pursuer, they add up to his sub-optimal play and allow evader (if evader has better maneuverability compared to that of pursuer) to come even more closer to the target than in simulations. Same is the case with the evader. If pursuer has faster turn rate than that of evader, evader path becomes sub-optimal and compensates

pursuer's sub-optimal play.

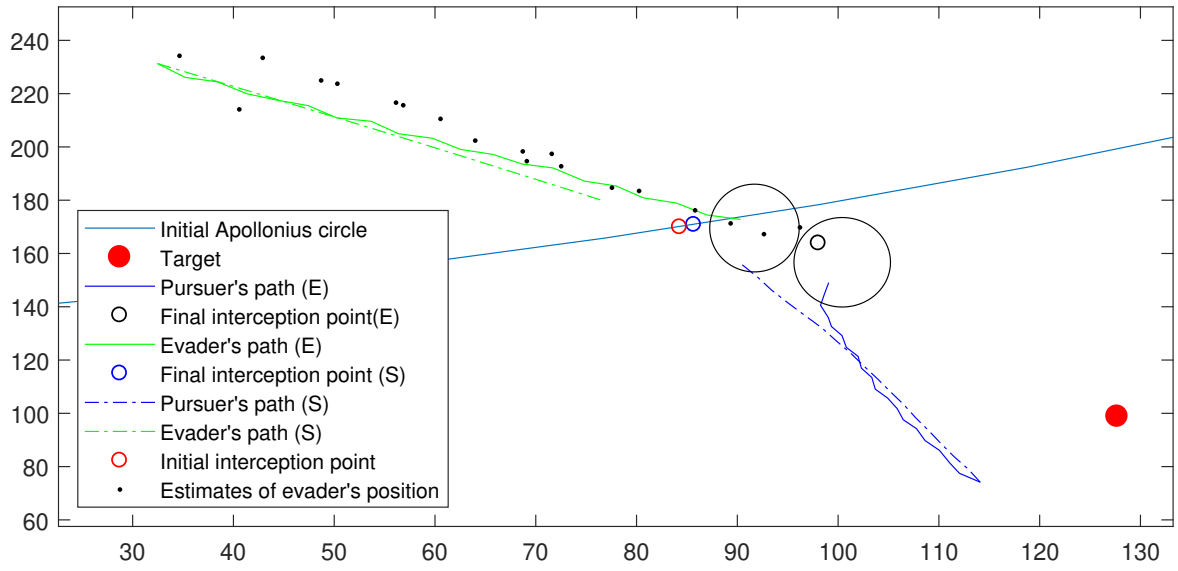

Figure 6.3: Experimental versus simulation results. Black circles indicate approximate sizes of robots

Figures 6.4a and 6.4b validate the satisfactory operation of the Kalman filter designed to estimate evader's position and speed. Like in simulations, Kalman filter was able to use the measurements of speed to improve the estimates. Measurements of states x_e, y_e were not useful much after $n = 6$ in improving corresponding estimates. But pursuer was able to intercept evader at a point close to initial interception point. So, if the initial distance between target and pursuer is small and target is in pursuer's dominance region, pursuer can win the game by pursuing interception point corresponding to estimates of evader's position and speed.

Similar experiments to validate the performance of $KF2$ were performed. As expected, experimental results showed that performance of $KF1$ is better than that of $KF2$. To avoid repetition, experimental results are not presented in this document.

6.4 Conclusion and future work

In this work, game geometry of target guarding problem was extensively studied. PSBNE of TGP was found. Algorithms for pursuer to follow in order to win the game when he is uncertain of evader's position and speed were proposed. Two Kalman

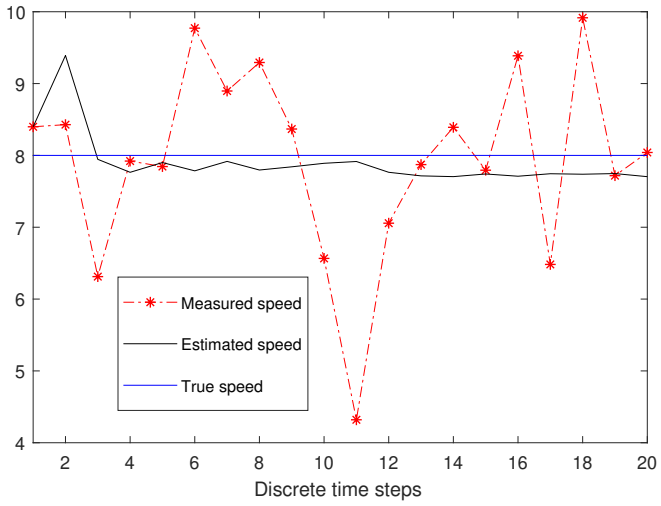

(a) plots of measured, estimated and true values of speed

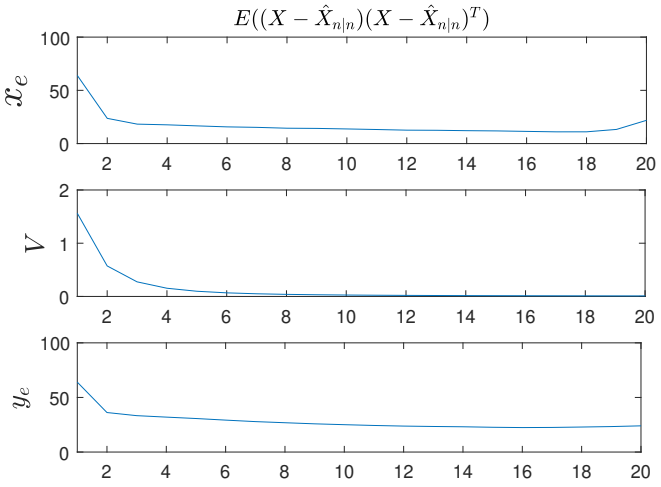

(b) Auto-covariance plots of the states

filters, one to estimate evader's position and speed and other to estimate interception point were designed. From results we argued that estimating evader's position and speed gives better results in terms of intercepting evader at farther distance from target. Probability density map of the interception point was found and performances of the pursuer's play when he pursues mean, most probable interception point and mean heading angle were studied.

No constraints on the target location in order for pursuer to win the game in-spite of his sub-optimal play have been determined. Hence, the future work points to finding bounds on minimum initial distance between target and evader in order to guarantee success for pursuer when measurements are associated with noise.

REFERENCES

[1] R. Isaacs. Differential Games: A Mathematical Theory with Application to Warfare and Pursuit, Control and Optimization. John Wiley and Sons, Inc. 1965.

[2] Raghav Harini Venkatesan Nandan Kumar Sinha. "The Target Guarding Problem Revisited: Some Interesting Revelations."

[3] R. Harini Venkatesan and N. K. Sinha, "A New Guidance Law for the Defense Missile of Nonmaneuverable Aircraft," in IEEE Transactions on Control Systems Technology, vol. 23, no. 6, pp. 2424-2431, Nov. 2015.

[4] D. Li and J. B. Cruz, "Defending an Asset: A Linear Quadratic Game Approach," in IEEE Transactions on Aerospace and Electronic Systems, vol. 47, no. 2, pp. 1026-1044, April 2011.

[5] D. W. Oyler and A. R. Girard, "Dominance regions in the Homicidal Chauffeur Problem," 2016 American Control Conference (ACC), Boston, MA, 2016, pp. 2494-2499.

[6] J. Fan, J. Ruan, Y. Liang and L. Tang, "An iterative learning process based on Bayesian principle in pursuit-evasion games," Proceedings of the 29th Chinese Control Conference, Beijing, 2010, pp. 52-55.

[7] P. Zarchan and H. Musoff, Fundamentals of Kalman Filtering: A Practical Approach. American Institute of Aeronautics and Astronautics, Virginia, 2000.

[8] Meir Pachter, Eloy Garcia, and David W. Casbeer. "Differential Game of Guarding a Target", Journal of Guidance, Control, and Dynamics, Vol. 40, No. 11 (2017), pp. 2991-2998.

APPENDIX A

Locations of evader and pursuer with respect to Apollonius circle

The equation of Apollonius circle is

$$(x - x_c)^2 + (y - y_c)^2 = R^2$$

where

$$x_c = \frac{x_e - x_p k^2}{1 - k^2}, y_c = \frac{y_e - y_p k^2}{1 - k^2} \tag{A.1}$$

$$R = \sqrt{x_c^2 + y_c^2 - \frac{x_e^2 + y_e^2}{1 - k^2} + k^2 \frac{x_p^2 + y_p^2}{1 - k^2}} \tag{A.2}$$

$$= \sqrt{\left(\frac{k}{1 - k^2}\right)^2 ((x_e - x_p)^2 + (y_e - y_p)^2)}$$

Let

$$D_e = (x_e - x_c)^2 + (y_e - y_c)^2 - R^2 \tag{A.3}$$

$$D_p = (x_e - x_c)^2 + (y_e - y_c)^2 - R^2 \tag{A.4}$$

Substituting (A.1), (A.2) in (A.3) leads to

$$D_e = \left(\frac{1}{1 - k^2}\right)^2 (x_e(1 - k^2) - (x_e - x_p k^2))^2 + (y_e(1 - k^2)$$
$$- (y_e - y_p k^2))^2 - \left(\frac{k}{1 - k^2}\right)^2 ((x_e - x_p)^2 + (y_e - y_p)^2)$$

$$= \left(\frac{1}{1 - k^2}\right)^2 \left((x_e - x_p)k^2\right)^2 + \left((y_e - y_p)k^2\right)^2 - (k)^2\left((x_e - x_p)^2 + (y_e - y_p)^2\right)$$

$$= \left(\frac{k^4 - k^2}{(1 - k^2)^2}\right)\left((x_e - x_p)^2 + (y_e - y_p)^2\right)$$

$$= \left(\frac{-k^2}{1 - k^2}\right)\left((x_e - x_p)^2 + (y_e - y_p)^2\right)$$

As $k^2\left((x_e - x_p)^2 + (y_e - y_p)^2\right)$ is a positive quantity, $D_e < 0$ if $k < 1$ and $D_e > 0$ if $k > 1$. This implies evader lies inside the Apollonius circle when his speed is less than pursuer's speed and lies outside the Apollonius circle when his speed is greater than the pursuer's speed.

In similar lines we can show that pursuer lies inside the Apollonius circle when his speed is less than evader's speed and lies outside the Apollonius circle when his speed is greater than the evader's speed.

APPENDIX B

Criterion for the existence of single evader point that results in the given interception point (when k is constant)

Speed ratio k is given by (2.27).

$$k^2(\theta) = \frac{(x_I - (x_{cm} + R_m\cos\theta))^2 + (y_I - (y_{cm} + R_m\sin\theta))^2}{(x_I - x_p)^2 + (y_I - y_p)^2}$$
$$= \frac{((x_I - x_{cm})^2 + (y_I - y_{cm})^2 + R_m^2 + 2(x_I - x_{cm})R_m\cos\theta + 2(y_I - y_{cm})R_m\sin\theta}{(x_I - x_p)^2 + (y_I - y_p)^2} \tag{B.1}$$

$$\frac{\partial(k^2(\theta))}{\partial\theta} = \frac{-2(x_I - x_{cm})R_m\sin\theta + 2(y_I - y_{cm})R_m\cos\theta}{(x_I - x_p)^2 + (y_I - y_p)^2}$$

$$\frac{\partial(k^2(\theta))}{\partial\theta} = 0 \Rightarrow \tan\theta = \frac{y_I - y_{cm}}{x_I - x_{cm}} \tag{B.2}$$

Substituting expressions of x_{cm}, y_{cm} from (2.18) in (B.2), we get

$$\tan\theta = \frac{-1}{M} = -\left(\frac{x_I - x_t}{y_I - y_t}\right) \tag{B.3}$$

Define $\theta_{max}, \theta_{min}$ as

$$\theta_{max} = \arg\max_{\theta} k_e(\theta)$$

$$\theta_{min} = \arg\min_{\theta} k_e(\theta)$$

From (B.2), $|\theta_{max} - \theta_{min}| = 180^0$

i.e., Line L (2.7) becomes tangent to circle C_e (2.9) when $k = \{k(\theta_{min}), k(\theta_{max})\}$.

Note that

$$k(\theta_{min}) = 0$$
$$x_e(\theta_{min}) = x_I \tag{B.4}$$
$$y_e(\theta_{min}) = y_I$$

APPENDIX C

Out of two elements of set S, the one that is farthest from target belongs to the set S_f

Let the elements of set S be $E_1(x_{e1}, y_{e1}), E_2(x_{e2}, y_{e2})$. Let C_1, C_2 be the Apollonius circles of E_1, E_2 respectively. Let the $O_1(a,0), O_2(b,0)$ be centers of C_1, C_2 respectively. From Appendix A we know that for $k < 1$, E_i lies inside C_i, $i = 1,2$. Let target $T(x_T, 0)$ be outside C_1.

Without loss of generality, we can assume $0 < x_T < x_I < b$. If $0 < x_T < a < x_I$, then $E_1 \in S_2$. If $0 < a < x_T < x_I$, then $E_1 \in S_1$ (refer Fig 2.4, 2.5 and definitions of S_1, S_2). E_2 belongs to set S_f.

$$(x_{e1} - x_I)^2 + (y_{e1} - y_I)^2 < (x_{e1} - x_T)^2 + (y_{e1} - y_T)^2 \quad \Rightarrow \quad E_2 \in S_2$$

$$(x_{e1} - x_I)^2 + (y_{e1} - y_I)^2 \geq (x_{e1} - x_T)^2 + (y_{e1} - y_T)^2 \quad \Rightarrow \quad E_2 \in S_1$$

I lies on C_1 and C_2. As C_e of (2.9) is a circle with center I and is constrained to pass through E_1 and E_2, E_2 lies outside C_1 and E_1 lies outside C_2. Note that I is equidistant from E_1 and E_2.

Let $I_f(x_{e1}, y_{e1}, k) = (x_I, y_I)$. As E_1 and E_2 satisfy equations (2.7), (2.9) $x_{e1} \leq x_I \leq x_{e2}$. $y_{e1} = y_{e2}$ as slope of line $\overline{TI}$ is equal to slope of $\overline{E_1E_2}$. So the inequalities (C.1), (C.2) hold

$$(x_{e2} - x_I)^2 + (y_{e2} - y_I)^2 \leq (x_{e2} - x_t)^2 + (y_{e2} - y_t)^2 \tag{C.1}$$

$$(x_{e1} - x_T)^2 + (y_{e1} - y_T)^2 \leq (x_{e2} - x_T)^2 + (y_{e2} - y_T)^2 \tag{C.2}$$

Inequality (C.2) means that the element of S that is farthest from target belongs to S_f.